Molecular Pharmacology Fast Forward. Published on September 15, 2009 as doi:10.1124/mol.109.059139
This article has not been copyedited and formatted. The final version may differ from this version.

SUBTYPE-SPECIFIC DIFFERENCES IN CRF RECEPTOR COMPLEXES DETECTED BY FLUORESCENCE SPECTROSCOPY

Laura Milan-Lobo[1], Ingrid Gsandtner, Erwin Gaubitzer, Dominik Rünzler, Florian Buchmayer, Gottfried Köhler, Antonello Bonci, Michael Freissmuth and Harald H. Sitte

Institute of Pharmacology, Center for Biomolecular Medicine and Pharmacology, Medical University Vienna, Austria (LML, IG, FB, MF, HHS)

Max F. Perutz Laboratories, University of Vienna, Austria (EG, DR, GK)

The Ernest Gallo Clinic and Research Center, Emeryville, and Department of Neurology, UCSF, CA, USA (AB).

Molecular Pharmacology Fast Forward. Published on September 15, 2009 as DOI: 10.1124/mol.109.059139
This article has not been copyedited and formatted. The final version may differ from this version.

Running title: Lateral mobility of CRF-receptors

Corresponding author: Michael Freissmuth, Medical University of Vienna, Center for Biomolecular Medicine and Pharmacology, Institute of Pharmacology, Waehringerstrasse 13a, A-1090 Vienna, Austria, Tel: +43-1-4277-64171, Fax: +43-1-4277-9641;

Email: michael.freissmuth@meduniwien.ac.at

Number of text pages: 33

Number of Figures: 12

Number of references: 40

Number of words in abstract: 239

Number of words in introduction: 588

Number of words in discussion: 1325

Abbreviations:

CFP, YFP, cyan and yellow fluorescent protein; CRF, corticotropin releasing factor; CRFRs, CRF receptors, C-SERT-Y, CFP-serotonin transporter-YFP; Y-DAT, YFP-dopamine transporter; FCS, fluorescence correlation spectroscopy; FIDA, fluorescence intensity distribution analysis; FRAP, fluorescence recovery after photobleaching; GPCR's, G protein-coupled receptors.

Molecular Pharmacology Fast Forward. Published on September 15, 2009 as DOI: 10.1124/mol.109.059139
This article has not been copyedited and formatted. The final version may differ from this version.

ABSTRACT

G protein-coupled receptors have been proposed to exist in signalosomes subject to agonist-driven shifts in the assembly-disassembly equilibrium, affected by stabilizing membrane-lipids and/or cortical actin restricting mobility. We investigated the highly homologous corticotrophin-releasing-factor receptors, CRFR1&2, which differ within their hydrophobic core. Agonist stimulation of CRFR1 and CRFR2 gave rise to similar to concentration-response curves for cAMP accumulation, but CRFR2 underwent restricted collision coupling. Both, CRFR1 and CRFR2, formed constitutive oligomers at the cell surface and recruited β-arrestin upon agonist activation (as assessed by fluorescence resonance energy transfer - FRET - microscopy in living cells). However, CRFR2 - but not CRFR1 - failed to undergo agonist-induced internalization. Similarly agonist binding accelerated the diffusion rate of CRFR2 only (detected by fluorescence recovery after photobleaching (FRAP) and fluorescence correlation spectroscopy - FCS) but reduced the mobile fraction, which is indicative of local confinement. Fluorescence intensity distribution analysis (FIDA) demonstrated that the size of CRFR-complexes was not changed. Disruption of the actin cytoskeleton abolished the agonist-dependent increase in CRFR2 mobility, shifted the agonist concentration curve for CRFR2 to the left and promoted agonist-induced internalization of CRFR2. Our observations are incompatible with an agonist-induced change in monomer-oligomer equilibrium, but they suggest an agonist-induced redistribution of CRFR2 into a membrane microdomain that affords rapid diffusion but restricted mobility and that is stabilized by the actin cytoskeleton. Our data show that membrane anisotropy can determine the shape and duration of receptor-generated signals in a subtype-specific manner.

Molecular Pharmacology Fast Forward. Published on September 15, 2009 as DOI: 10.1124/mol.109.059139
This article has not been copyedited and formatted. The final version may differ from this version.

Introduction

Signal transduction via heterotrimeric G proteins is accomplished by a cycle of activation and deactivation of the Gα-subunit, which are achieved by receptor-catalyzed exchange of prebound GDP for GTP and GTP-hydrolysis by the intrinsic GTPase of Gα, respectively. Superimposed on this GTPase cycle, there is a cycle of subunit dissociation and reassociation, where the inactive heterotrimer Gα.GDP.βγ affords receptor docking, GTP binding drives subunit dissociation into Gα.GTP.Mg^{2+} and Gβγ and the GTPase-mediated hydrolysis promotes mutual inactivation of two Gα.GDP and Gβγ by reassociation of the inactive heterotrimer Gα.GDP.βγ. This model has been established some 20 years ago, mainly by the study of reconstituted purified components (Freissmuth *et al.*, 1989). However, subsequently, methods have become available, which allow to track the activity of individual components at the single cell level. In several instances, these have led to observations which are incompatible with some of the central tenets of the model or which require the model to be adapted. For some receptors, it has been questioned, whether subunit dissociation occurs to any appreciable extent in intact cells (Hein *et al.*, 2005). In addition, several G protein-coupled receptors have been found to form homo- and hetero-oligomers (reviewed in Pin et al., 2007). In some studies, the equilibrium between monomers and dimers has been shown to be regulated by receptor activation (Cvejic and Devi, 1997; Cheng and Miller, 2001; Briddon et al., 2004). Agonist-induced changes in diffusion have been viewed as evidence for an agonist-induced disassembly of large receptor aggregates. Finally, receptors and G proteins have been found to be inhomogeneously distributed over the cell surface (Perez *et al.*, 2006), because they may be clustered by association with anchoring molecules or trapped in specific membrane microdomains arising from the different miscibility of lipids (Chini and Parenti, 2004). It has, however, not been clear why some receptors should depend on cholesterol or on cholesterol-containing domains, while others don't.

Molecular Pharmacology Fast Forward. Published on September 15, 2009 as DOI: 10.1124/mol.109.059139
This article has not been copyedited and formatted. The final version may differ from this version.

We recently observed that the restricted mobility of the A_{2A}-receptor was a property specified by its hydrophobic core and contingent on the presence of cholesterol (Charalambous *et al.*, 2008). This observation predicts that closely related receptors may differ with respect to their mobility provided that their hydrophobic cores differ in their ability to accommodate cholesterol (or other lipids). Here, we have tested this hypothesis by examining the receptors for corticotropin releasing factor (CRF), which belong to the secretin-receptor-like family or B-family of GPCRs (Fredriksson *et al.*, 2003). Upon binding of their endogenous ligand CRF, they preferentially engage Gαs and thus activate adenylyl cyclase isoforms. At high occupancy, CRFRs can also activate additional G proteins (Wietfeld *et al.*, 2004). CRFRs are highly related with 74% identity and 88% homology; dissimilarities are not evenly distributed; surprisingly large degrees of divergence are observed within the transmembrane (TM) segments 1 to 4. Based on these differences, we surmised that these two receptor isoforms differed in the extent to which they formed complexes and diffused through the membrane. This conjecture was examined by recording the mobility of receptors at the ensemble level using fluorescence recovery after photobleaching (FRAP) and at the level of the individual molecule using fluorescence correlation spectroscopy (FCS) and fluorescence intensity distribution analysis (FIDA). Agonist occupancy enhanced the mobility of CRFR2 in the presence of an intact cytoskeleton. By contrast with CRFR1, CRFR2 underwent restricted collision coupling and greatly delayed internalization; disruption of the cytoskeleton by latrunculin A enhanced cAMP formation and promoted rapid internalization. Taken together, these results support a model where the mobility of the agonist-liganded CRFR2 is restricted by actin-dependent membrane anisotropy.

Molecular Pharmacology Fast Forward. Published on September 15, 2009 as DOI: 10.1124/mol.109.059139
This article has not been copyedited and formatted. The final version may differ from this version.

MATERIALS AND METHODS

Reagents. Vectors pECFP-N1 and pEYFP-N1 were from Clontech. Human/rat CRF, and alpha-helix CRF[9-41] were from Polypeptide (Wolfenbüttel, Germany). [^{125}I]sauvagine was from Perkin Elmer-NEN (Boston, MA). Rabbit polyclonal GFP antibody [632377] was from Clontech (Mountain view, CA, USA), anti-rabbit IgG1 (HRP) horseradish was from Amersham (Freiburg, Germany).

The sources of all other reagents and chemicals can be found in Charalambous *et al*. (2008).

cDNA constructs and cell culture. The plasmid coding for mouse CRFR2β and CRFR1α were kindly provided by W. Vale (La Jolla, USA) and P. Ferrara (Basel, Switzerland), respectively. cDNAs were subcloned into pECFP-N1 and pEYFP-N1 to attach the FP at the C-terminus; the integrity of all constructs was verified by sequencing. Rab5-CFP was kindly provided by Alexander Sorkin (University of Colorado, Colorado, USA). β-arrestin2-YFP was kindly provided by Martin Lohse (Institute of Pharmacology and Toxicology and Bio-Imaging Center, University of Würzburg, Würzburg, Germany).

HEK293 cells were transiently or stably transfected by the Ca_2PO_4-precipitation method. For experiments employing Rab5, cells stably expressing CRFR2-YFP or CRFR1-YFP were transiently transfected with Rab5-CFP. In the case of FRET experiments, all cDNAs were transiently transfected into parental HEK293 cells. Neuronal cultures were generated from hippocampi of neonatal Sprague-Dawley rats and transfected with Lipofectamine2000 (Invitrogen) after 7 days in culture.

Determination of cAMP formation and [^{125}I]sauvagine binding. The formation of [^{3}H]cAMP was quantified as previously described (Kudlacek *et al.*, 2001). The production of cAMP was stimulated by the addition of different CRF concentrations for 30 min at 37°C. membranes were prepared from HEK293 cells stably expressing CRFR1 and CRFR2 as in Kudlacek et al. (2001). Nuclei were removed by centrifugation (10 min at 1000 g). Membranes were harvested at 40,000 g for 30 min. Binding was done in a final volume of 0.1mL containing 50

Molecular Pharmacology Fast Forward. Published on September 15, 2009 as DOI: 10.1124/mol.109.059139
This article has not been copyedited and formatted. The final version may differ from this version.

mM Tris.Hcl, pH 7.5, 1 mM EDTA, 5 mM $MgCl_2$, 0.2 nM [^{125}I]sauvagine and membrane protein (2 to 4 µg) for 2 to 90 min at temperatures ranging from 20 to 37°C. The reaction was terminated by filtration over GFA filters that had been presoaked in 1% polyethleneimeine to reduce filter binding. Non-specific binding wass defined in the presence of the antagonist alpha-helix CRF[9-41]. Total binding was 4000-6000 cpm, non-specific binding amounted to ~1000 cpm and was mainly due to filter binding. Some incubations were also done in the presence of 0.1 mM GTPγS.

Fluorescence spectroscopy. FRET microscopy was performed applying the "three-filter method" essentially as described recently (Bartholomaeus *et al.*, 2008). FRAP was recorded on a Zeiss LSM510 confocal laser scanning microscope as described (Charalambous *et al.*, 2008). To allow better comparison, we determined the diffusion coefficient (D) using : $t_{1/2} = \beta\omega^2/4D$, where $t_{1/2}$ is the half-life of fluorescence recovery, ω the radius of the ROI and β is a parameter which depends on the percentage bleached (Yguerabide *et al.*, 1982). In all measurements β was set to 1.6, its maximum value (Yguerabide *et al.*, 1982). All measurements were done at 22°C. The setup and cell handling for FCS has been described in detail elsewhere (Maier *et al.*, 2005). In brief, we seeded stably transfected HEK293 cells expressing YFP-tagged CRFRs onto poly-D-lysine coated LabTek chamber slides. YFP was excited at 488 nm (Ar-laser line attenuated by optical density filters to avoid photobleaching, and a dichroic mirror with bandpass filters). The pinhole diameter was set to 45 µm (confocal volume element, horizontal radius ω_1 = 0.185 µm, as calibrated with rhodamine 6G ($D=2.8 \times 10^{-10}$ cm^2/s). Cells were first scanned in z-direction to identify two fluorescence peaks corresponding to the upper and the lower cell surface. All measurements were subsequently recorded at the upper membrane during 10 seconds and at 22°C. The autocorrelation function was obtained and fitted to the equation describing a two-component model with two diffusion times τ1 and τ2 (Maier *et al.*, 2005). The diffusion coefficient (D) was calculated from the relation: $\tau_D = \omega_1^2/4D$. FIDA was measured using the same FCS-set up; to obtain photon

Molecular Pharmacology Fast Forward. Published on September 15, 2009 as DOI: 10.1124/mol.109.059139
This article has not been copyedited and formatted. The final version may differ from this version.

arrival times the detector signal was split and guided into the correlator card and into a time measurement histogram accumulating real-time processor (Timeharp 200; Picoquant, Germany) triggered with 7.4 MHz. The recorded photons were binned into 40 µs time windows. Photon counting histograms were generated based on the probability for the occurrence of photon counts. The probability distributions were analyzed using the FIDA model according to (Kask *et al.*, 1999). The resulting brightness values relate to the tailing of the distribution on the side of higher photon counts. Details on the analysis and the calculation of the brightness can be found in equation 3 (Edetsberger *et al.*, 2005).

Statistical analysis: All data samples were first tested for normal distribution using the Kolmogorow-Smirnow-test. Subsequently, we applied ANOVA followed by post hoc-Bonferroni´s test for multiple comparisons (Fig. 2). Alternatively, if the criteria of the Kolmogorow-Smirnow-test were not met, we used the non-parametric Kruskal-Wallis test with a post hoc-comparison of all column pairs (Figs. 4, 5, 7). Where appropriate, we used unpaired (Fig. 8) and paired t-test (Fig. 11).

Molecular Pharmacology Fast Forward. Published on September 15, 2009 as DOI: 10.1124/mol.109.059139
This article has not been copyedited and formatted. The final version may differ from this version.

RESULTS

CRF receptors engage G_s and G_i, form oligomers, recruit β-arrestin but differ in their ability to undergo internalization. We generated stably transfected HEK 293 cell lines that expressed fluorescently tagged CRFRs at comparable levels. These receptors were functionally indistinguishable from untagged receptors (data not shown); the concentration-response curves for the physiological agonist were comparable; most notably, we observed that in both, CRFR1 (Fig. 1A) and CRFR2 (Fig. 1B) the concentration-response curve for agonist-induced cAMP accumulation was bell-shaped. The decline observed at high concentrations of CRF was blunted in cells that had been pretreated with pertussis toxin. This indicates that the receptor preferentially engages Gs but that Gi-isoforms (and possibly other G proteins) are also recruited at high agonist occupancy. Oligomer formation of CRFR1 and CRFR2 was investigated in living cells by FRET microscopy. CFP- and YFP-tagged receptors were transiently co-expressed in appropriate combinations; only cells displaying a CFP/YFP ratio of ~1 (mean value=1.0±0.2) were included in the analysis of N_{FRET}. We controlled our FRET measurements by (i) co-expression of (soluble) CFP and YFP as negative control, and (ii) a dually tagged serotonin transporter, C-SERT-Y (Just *et al.*, 2004), as positive control. CFP and YFP displayed low background FRET (N_{FRET}=0.08±0.08; mean±SD), whereas C-SERT-Y, as expected, gave a strong FRET (N_{FRET}=0.60±0.15). Energy transfer was observed between CRFR1-C and CRFR1-Y (N_{FRET}=0.23±0.10), as well as CRFR2-C and CRFR2-Y (0.35±0.14; Fig. 2B). As a negative control for membrane crowding, we coexpressed CFP-tagged CRFRs and the structurally unrelated YFP-tagged dopamine transporter (DAT). These gave low N_{FRET} (CRFR1-C/YFP-DAT: 0.06±0.09 and CRFR2-C/YFP-DAT: 0.13±0.04; Fig. 2B) comparable to the background FRET of CFP/YFP (Fig. 2B).

While it is clear that monomeric receptors are in principle capable of activating a G protein (Ernst et al., 2007; Whorton et al., 2007); however, there are several examples where G protein activation is contingent on the dimeric form of the receptor (Brock et al., 2007;

Molecular Pharmacology Fast Forward. Published on September 15, 2009 as DOI: 10.1124/mol.109.059139
This article has not been copyedited and formatted. The final version may differ from this version.

Hlavackova et al., 2005). It was therefore conceivable that receptor occupancy promoted receptor dimerization. Accordingly, we treated HEK293 cells coexpressing CRFR1-C/CRFR1-Y and CRFR2-C/CRFR2-Y with CRF: agonist challenge did not change FRET within the CRFR1 oligomer (Fig. 2C). In contrast, FRET significantly increased in CRFR2 ($p<0.001$) upon agonist stimulation (Fig. 2C). This was specific: incubation with the antagonist α-helical CRF[9-41] (αhCRF) did not alter N_{FRET} (data not shown). We stress, however, the change in the FRET-signal of CRFR2 oligomers may either be due to a change in the distance and/or relative orientation of the fluorophores resulting from the agonist-induced conformation or from an agonist-induced increase receptor oligomers (see FIDA below).

We employed FRET microscopy to verify that agonist stimulation of both, CRFR1 and CRFR2 resulted in the recruitment of β-arrestin-1; it is evident from Fig. 3A that there was no appreciable difference between these two receptors (Fig. 3A). However, while agonist challenge promoted internalization of CRFR1 into Rab5-positive endosomes (Fig. 3B, top row), CRFR2 was remarkably resistant to internalization: up to 45 min, after agonist challenge, there were only occasional internalization events (Fig. 3B) bottom row. We stress that the observation period covered very early time points and that there was no evidence for early internalization followed by rapid recycling; more pronounced internalization of CRFR2 was only seen after incubations exceeding 60 min (not shown). Thus CRFR1 and CRFR2, appeared to activate similar G proteins and to both recruit β-arrestin, nevertheless they differed with respect to internalization and to the nature of the oligomeric complex.

Mobility of the CRFR complexes at the plasma membrane monitored by FRAP. The agonist-induced increase in FRET of CRFR2 may have resulted from (i) increased accumulation of CRFR2 in oligomeric complexes or (ii) from a decline in fluorophore distance and/or rotational mobility in existing oligomers. An increase in the size of the oligomeric complex

Molecular Pharmacology Fast Forward. Published on September 15, 2009 as DOI: 10.1124/mol.109.059139
This article has not been copyedited and formatted. The final version may differ from this version.

ought to result in a change in mobility. We tested this possibility by comparing the mobility of YFP-tagged CRFR1 and CRFR2 stably expressed in HEK293 cells by FRAP. The fluorescence was uniformly distributed over the cell surface. A membrane strip of ~5 µm was photo-bleached and recovery of fluorescence was monitored to estimate the lateral mobility of the receptors (Fig. 4B). In the absence of agonist, CRFR1 and CRFR2 did not differ in their mobility: maximal recovery was about 60% of pre-bleach values (empty symbols in the bottom panels of Fig. 4B); and half-maximal recovery was achieved after ~15 s resulting in a diffusion coefficient of $2.3\pm0.9 \times 10^{-9}$ cm^2/s and $2.3\pm0.8 \times 10^{-9}$ cm^2/s for CRFR1 and CRFR2, respectively (mean ± SD; Fig. 3B). Then, cells were incubated with different concentrations of the agonist CRF for 15 min. During this time and with the highest concentration employed (100 nM), some internalization was seen for CRFR1, but the bulk of the receptors were still present at the plasma membrane to allow for fluorescence recovery (see Fig. 4B). In contrast, CRFR2 did not internalize during the first 40 min of agonist challenge (see Fig. 3B). Accordingly, all recordings were done within 15 min of agonist challenge to minimize confounding effects arising form internalization. Agonist-activation did not significantly affect the diffusion coefficient of CRFR1 (Fig. 4B, left panel). In contrast, agonist activation of CRFR2-Y significantly increased the diffusion coefficient (Fig. 4B, right panel). This effect was specific for the agonist because a saturating concentration of antagonist did not affect the mobility of CRFR2-Y (Fig. 4B, right panel). Cells were pretreated for 1 h with latrunculin A to disrupt cortical actin filaments: this manipulation did not affect the lateral mobility but abolished the agonist-induced increase in mobility of CRFR2 (Fig. 4B, right panel). Agonist activation of CRFRs also affected the extent of maximal fluorescence recovery, i.e., the mobile fraction (Fig. 4C). This effect was most pronounced for CRFR2-Y: a statistically significant decrease in the mobile fraction was seen in the presence of both, 10 and 100 nM CRF, but not in the presence of the antagonist or of latrunculin A (Fig. 4C, right panel). However, the mobile fraction of CRFR1 also decreased in a statistically significant

Molecular Pharmacology Fast Forward. Published on September 15, 2009 as DOI: 10.1124/mol.109.059139
This article has not been copyedited and formatted. The final version may differ from this version.

manner in the presence of CRF (Fig. 4C, left panel). This drop may be rationalized by taking into consideration the agonist-induced internalization of CRFR1, but it is not readily evident why the mobile fraction of CRFR2 should decrease upon agonist occupancy because this receptor did not internalize to an appreciable extent (Fig. 3B). Finally, it is also worth mentioning that fractional recovery was lower in CRFR2 than in CRFR1.

Diffusion coefficient for CRFR subtypes determined by FCS. The FRAP experiments summarized above indicated that agonist stimulation (i) increased the mobility of CRFR2 and, in addition, (ii) caused immobility of at least some of these complexes. FRAP analysis only allows for a global estimate of protein mobility, because it averages the movement of a large number of molecules, i.e. ensemble behavior. Hence, it does not allow to understand the distribution of mobilities of individual fluorescent species: this was explored by employing FCS (Bacia and Schwille, 2003; Chen et al., 2006). For FCS measurements, the confocal volume was positioned at the upper membrane of a HEK293 cell stably expressing CRFR1 or CRFR2; the fluctuations in fluorescence were recorded for 10 seconds. The analysis of the resulting autocorrelation curves for CRFR1 (Fig. 5A, left) and for CRFR2 (Fig. 5A, right) revealed that the data were best described by a model assuming the presence of two fluorescent species. The first component revealed a diffusion time ($\tau 1$) of ~0.15 ms; this is too fast for a membrane protein (Adkins et al., 2007; Barak et al., 1997). Such rapidly diffusing species are commonly observed in FCS microscopy and most likely correspond to “on/off” fluorescence flickering of free YFP molecules (Haupts et al., 1998; Philip et al., 2007; Pucadyil et al., 2004). Free YFP molecules were indeed detected in cell lysates (see below, Fig. 7B). In contrast, the second component ($\tau 2$) extracted from the generating function was consistent with the (membrane-embedded) fluorescently tagged CRFR complex: It is evident from Fig. 4B that there was a large variation in the mobility of individual fluorescent receptor species in both, CRFR1 and CRFR2 expressing cells. On average, rapidly moving species of

Molecular Pharmacology Fast Forward. Published on September 15, 2009 as DOI: 10.1124/mol.109.059139
This article has not been copyedited and formatted. The final version may differ from this version.

CRFR1 were slightly more abundant than of CRFR2 under basal condition. However, increasing concentrations of CRF augmented the proportion of rapidly moving CRFR2-Y, resulting in a significant increase in average mobility (e.g., diffusion coefficient D_2 of CRFR2=5.8±3.4 × 10^{-9} cm^2/s in the presence of 100nM CRF; Fig. 5B, right panel). This effect was contingent on the agonist activity of CRF: it was not elicited by saturating concentrations of the antagonist which, however, blocked the CRF effect (D_2=5.7±3.9 × 10^{-9} cm^2/s). CRF specifically affected the mobility CRFR2 because it did not alter the relative distribution of rapidly and slowly moving CRFR1 species (Fig. 5B, left panel). Analogous data were obtained in hippocampal neurons expressing CRFRs (Fig. 6). We noted that the diffusion rate in hippocampal neurons was consistently faster than in HEK293 cells (*cf.* Figs. 5 & 6). For obvious reasons, hippocampal neurons were transiently transfected to express the receptors. We therefore verified that the level of CRFR expression did not affect the lateral mobility. We compared three different cell lines stably expressing CRFR2; the expression level in these cells varied >>20-fold requiring different exposure times to visualize the immunoreactive bands (Fig. 7B); the range of expression of CRFR2 comprised the expression level of CRFR1 (right hand lane labelled #4 in Fig. 7B). In spite of this large variation in expression level, the FCS recordings were virtually surperimposable. (Fig. 7A). It is also evident that immunoreactive degradation products were present, most notably a band at 25 kDa corresponding to free YFP (open arrow in Fig. 7B), which - as mentioned earlier - accounted for the rapidly diffusing component resolved in the generator function.

The agonist-induced shift in mobility of CRFR2 is contingent on cortical actin filaments and cholesterol. CRFR1 and CRFR2 are thought to regulate identical effectors; however, it is conceivable that the mobility of a large proportion CRFR2 is locally confined by the cytoskeleton, i.e. cortical actin filaments. In this model, agonist stimulation of CRFR2 generates a signal that reshapes the cytoskeleton and thus allows for rapid diffusion of

Molecular Pharmacology Fast Forward. Published on September 15, 2009 as DOI: 10.1124/mol.109.059139
This article has not been copyedited and formatted. The final version may differ from this version.

previously immobile receptors. In FRAP experiments, the basal mobility of CRFR2-Y was not affected by treating the cells with latrunculin A. Both, the diffusion coefficient (Fig. 4B, right panel) and the mobile receptor fraction (Fig. 4C, right panel), were similar to those observed under control conditions. FRAP records ensemble changes in mobility; given the large variation in individual mobilities (see Fig. 5), it is not surprising that FRAP is less sensitive than FCS. Accordingly, we also assessed the effect of latrunculin A on receptor mobility by FCS: lateral mobility of the receptors was not affected *per se*, but it abrogated the agonist-induced appearance of rapidly moving species. Hence the average mobility was unchanged (Fig. 8B). These observations are inconsistent with receptor-induced remodelling of actin filaments but they are indicative of a more fundamental source of membrane anisotropy and/or receptor heterogeneity, *i.e.* one that cannot be solely accounted for by microdomains created by the submembraneous cytoskeleton.

Cholesterol is thought to be distributed inhomogeneously over the membrane. A possible contribution thereof was tested by depleting or clustering cholesterol with methyl-β-cyclodextrin and filipin3, respectively. Pretreatment of cells with these substances caused a significant shift in the distribution of CRFR2 mobility with a preponderance of slowly migrating species resulting in low average diffusion coefficients (Fig. 8). Importantly, stimulation with CRF did not result in an increase in the lateral mobility of CRFR2 under these conditions (Fig. 8B). Readdition of cholesterol antagonized the actions of methyl-β-cyclodextrin (data not shown, see Charalambous et al., 2008). We also attempted to resolve different populations of receptors by density gradient centrifugation. However, while it was possible to isolate detergent resistant-membranes (*i.e.*, membrane proteins resistant to extraction by triton X-100) on sucrose gradients, these failed to reveal a different distribution of CRFR1 and CRFR2 regardless of whether the cells were stimulated with agonist or preincubated with antagonist prior to cell lysis (data not shown).

Molecular Pharmacology Fast Forward. Published on September 15, 2009 as DOI: 10.1124/mol.109.059139
This article has not been copyedited and formatted. The final version may differ from this version.

Changes in lateral mobility are not accounted for by changes in size of CRFR2 receptors. The higher lateral mobility of CRFR2 receptors observed after ligand binding cannot explain the results obtained by FRET microscopy: agonist incubation augmented FRET in CRFR2 homo-oligomers. One possible explanation is to assume increased accumulation of CRFR2 in oligomeric complexes. The changes in mobility (recorded by FRAP and FCS) provided circumstantial evidence against this explanation. The alternative interpretation is to posit that the oligomeric nature of the receptor is not affected by agonist treatment but the mobility is altered by the agonist because the receptor complexes are released, e.g., from tethering molecules or redistributed into membrane areas with increased fluidity. The two hypothetical explanations can be differentiated by employing fluorescent intensity distribution analysis (FIDA; Fig. 9) because the number of photons emitted by a diffusing entity is determined by its number of fluorophores (Kask *et al.*, 1999). Accordingly, the presence of two species of distinct size ought to be reflected in the distribution of emitted photons over time. However, the photon counting histograms depicted in Fig. 9 were all adequately described by a probability distribution for a single species: regardless of whether the cells had been incubated in the absence (Fig. 9A, top panels) or presence of agonist (Fig. 9A, bottom panels), the fit was not improved by assuming the presence of a second species and this was true for both CRFR isoforms (Fig. 9B).

CRFR1 and CRFR2 differ by their mode of coupling - restricted versus unrestricted collision coupling. Taken together, the observations are consistent with the following hypothetical model: CRFR2 undergoes an agonist-induced redistribution into a membrane compartment that allows for fruitful coupling with its cognate G proteins(s). Gs is thought to be also subject to anisotropic distribution in the plasma membrane (Allen et al., 2007). In the agonist-liganded state, the long range mobility of CRFR2 may be restricted by the actin cytoskeleton. In contrast, CRFR1 may sample the large areas of the membrane with unrestricted mobility.

Molecular Pharmacology Fast Forward. Published on September 15, 2009 as DOI: 10.1124/mol.109.059139
This article has not been copyedited and formatted. The final version may differ from this version.

Experiments designed to test the mode of G protein-coupling are carried out under cell culture conditions, i.e. at 37°C; FCS recordings and FRAP experiments, however, were done at 22°C. Depending on the lipid composition of the membrane, it is conceivable that the fluidity of the membrane changes over this temperature range and this may affect signal transfer from receptor via G protein to the effector (Whetton et al., 1983). With our setups, it has not been possible to record receptor mobility at 37°C: temperature gradients resulted in abrupt and unpredictable shifts in the focus plane. As an alternative, we examined receptor-G protein coupling at different temperatures by employing high-affinity agonist binding (which is contingent on ternary complex formation of agonist-receptor and G protein see Freissmuth et al., 1989). CRFR1 and CRFR2 were labeled with the high-affinity agonist [^{125}I]sauvagine and the association rate was determined at temperatures ranging from 20°C to 37°C (shown for CRFR1 in Fig. 10A). Binding was greatly reduced by addition of GTPγS (open triangle in Fig. 10A) indicating that binding tracked ternary complex formation. It is evident from Fig. 10B that the Arrhenius plot was linear over the temperature range studied, there was no evidence for a break point that would be indicative of a phase transition. Finally, the slopes of the Arrhenius plots were in a range to those determined previously (Waldhoer et al., 1999).

The model of distinct mobilities of CRFR1 and of CRFR2 posits that - because of its restricted mobility - CRFR2 may only interact with G proteins in its close vicinity resulting in restricted collision coupling. We used two approaches to this model: (i) we varied receptor expression levels and (ii) we examined the effect of disrupting the actin cytoskeleton on the agonist-induced response. The expression level of CRFR2 and CRFR1 was varied 5-fold and the agonist-induced cAMP accumulation was measured in pertussis toxin-treated cells to obviate confounding effects arising from the recruitment of Gi at high agonist occupancy (*cf.* Fig. 1). In restricted collision coupling, increased levels of receptor expression translate solely into an increased maximum effect (E_{max}). In contrast, the EC_{50} for the agonist does not

Molecular Pharmacology Fast Forward. Published on September 15, 2009 as DOI: 10.1124/mol.109.059139
This article has not been copyedited and formatted. The final version may differ from this version.

change, because of the limited number of G proteins engaged by a spatially restricted receptor. However, increased receptor levels translate into a leftward shift of the concentration response curve for the agonist due to the built-in signal amplification of unrestricted collision coupling. It is evident from Fig. 11 that agonist potency, i.e. EC_{50} for CRF, varied with the expression level of CRFR1 (Fig. 11A), but not with CRFR2 (Fig. 11B). Conversely, disrupting the cytoskeleton with latrunculin increased the response to CRFR2 receptor in the intermediate concentration-range (Fig. 11D) but did not affect the concentration-response curve for agonist at CRFR1 (Fig. 11C). Microtubules are also thought to participate in the organization of signaling complexes (Allen et al., 2007). Disruption of microtubuli by the depolymerizing agent colchicine, for instance has been shown, to blunt adenylyl cyclase stimulation via G_s (Head et al., 2006). As shown in the inset to Fig. 11C&D, this can also be recapitulated with CRF-mediated cAMP-accumulation; however, signal transfer from CRFR1 and CRFR2 is impaired to a similiar extent. We stress that the experiments summarized in Fig.11C&11D were carried out in stably transfected cells that expressed equivalent levels of receptors.

Disrupting the actin cytoskeleton promotes internalization of CRFR2.

Upon binding of agonist CRFR2 recruits β-arrestin but fails to undergo internalization; we surmised that this deficiency was linked to the altered mobility of the agonist-liganded receptor, because the receptor entered into a compartment that shielded it from the internalization machinery. Accordingly, we pretreated stably transfected cells that expressed equivalent levels of CRFR1 and CRFR2 and challenged these with agonist. As expected, internalization of CRFR1 was seen in both, the absence (Fig. 12, top row) and presence (Fig. 12, second row) of latrunculin. Likewise, agonist stimulation did not trigger internalization CRFR2 under control conditions (Fig. 12, third row). In contrast, in latrunculin-treated cells (Fig. 12, bottom row), CRFR2 was as rapidly and as efficiently internalized as CRFR1. Thus,

Molecular Pharmacology Fast Forward. Published on September 15, 2009 as DOI: 10.1124/mol.109.059139
This article has not been copyedited and formatted. The final version may differ from this version.

the phenotypic differences between CRFR2 and CRFR1 were eliminated by disrupting the cytoskeleton.

Molecular Pharmacology Fast Forward. Published on September 15, 2009 as DOI: 10.1124/mol.109.059139
This article has not been copyedited and formatted. The final version may differ from this version.

DISCUSSION

It is generally accepted that GPCRs can exist both, in monomeric and oligomeric form, but it has remained contentious whether agonists affect the monomer-oligomer equilibrium (Pfleger and Eidne, 2005). There are two approaches that have been employed to address the issue: (i) methods that focus on changes in resonance energy transfer between fluorescently labeled receptor moieties. Increases or decreases in resonance energy transfer, however, do not provide any unequivocal evidence for a change in the oligomer/monomer equilibrium, because energy transfer does not only depend on the distance of the fluorophores but on their relative orientation and their rotational freedom. This information is accessible by measuring recording polarized light emission. A systematic survey shows that this has not been employed to differentiate between agonist-induced changes in monomer/dimer equilibrium and agonist-induced conformational changes (Pfleger and Eidne, 2005). (ii) Alternatively, the mobility of the receptor particle can be tracked. An accelerated mobility is typically viewed as evidence for a dissociation of large complexes, e.g., of the δ-opioid receptors (Cvejic and Devi, 1997). Conversely, the formation of higher order oligomers has been ascribed to a slowly diffusing receptor population (Philip *et al.*, 2007). Our observations do not support any of these interpretations for CRF receptors: analysis of brightness by FIDA unequivocally demonstrates that the size of the receptor species remains constant irrespective of the presence or absence of agonist. Several arguments suggest that a change in oligomeric assembly could have been detected in our experiments, if it had occurred: (i) CRFR1 and CRFR2 were present as oligomers at the plasma membrane; (ii) CRF enhanced FRET in CRFR2; (iii) FCS detected a large variation in the mobility of individual fluorescent receptor molecules; (iv) agonist activation induced a clear-cut shift in this distribution of CRFR2 diffusion rates. Thus, we conclude that CRFRs are constitutive oligomers of fixed stoichiometry, which is not subject to agonist regulation. This interpretation is in line with the current evidence that

Molecular Pharmacology Fast Forward. Published on September 15, 2009 as DOI: 10.1124/mol.109.059139
This article has not been copyedited and formatted. The final version may differ from this version.

suggests that the oligomeric state of secretin receptor-like/class B GPCRs is not subject to regulation by agonist occupancy (Pfleger and Eidne, 2005).

While CRFR1 and CRFR2 are closely related and couple to the same set of G proteins, they differed in their response to CRF in three respects: (i) agonist-induced changes in receptor mobility were only seen with CRFR2 but not with CRFR1; (ii) CRFR1 but not CRFR2 was internalized upon agonist binding; (iii) The EC_{50} for agonist activation of CRFR2 was independent of receptor levels, a finding consistent with restricted collision coupling. We argue that all three phenomena are related and provide circumstantial evidence for the conjecture that upon agonist- binding CRFR2 enters a different membrane microdomain where its movement is spatially restricted. These membrane domains are maintained by the actin cytoskeleton: upon entering into this microdomain, agonist-bound CRFR2 diffuses more rapidly but within a limited range: this interpretation is supported by the observation that agonist binding reduced the mobile fraction of CRFR2 which was prevented by latrunculin pretreatment. Accordingly, agonist-liganded CRFR2 has only access to a limited number of G_s molecules and is spatially segregated from the internalization machinery. Hence, it fails to undergo internalization although β-arrestin is readily recruited to CRFR2. Alternatively, CRFR2 may fail to undergo internalization, because it is tethered to the actin cytoskeleton, which can limit the propensity of receptors to undergo internalization (Puthenveedu and von Zastrow, 2006). This alternative explanation is unlikely, because it cannot account for the agonist-induced accelerated diffusion rates.

Agonist stimulation increased the diffusion rate of CRFR2 but not of CRFR1. This was uniformly seen regardless of whether FCS or FRAP were used. Different responses have also been noted previously: lateral mobility of A_{2A}-adenosine receptors was not affected upon receptor activation, while agonist treatment (i) decreased that of the D_2-receptor

Molecular Pharmacology Fast Forward. Published on September 15, 2009 as DOI: 10.1124/mol.109.059139
This article has not been copyedited and formatted. The final version may differ from this version.

(Charalambous *et al.*, 2008) and (ii) increased the mobility of the 5-HT_{1A}-receptor (Pucadyil et al., 2004). It is not clear, why receptor mobility changes in an unpredictable way upon agonist occupancy. FCS allowed us to extract information on the mobility of single receptors and showed that the diffusion coefficients varied widely. The basis for this anisotropy is also not clear, but it is indicative of some local confinement of receptors: hypothetical lipid rafts are obvious candidates. Both, G protein-coupled receptors (Perez et al., 2006) and G proteins have been found to be enriched in microdomains (Abankwa and Vogel, 2007); most importantly, these microdomains have been found to be substantially more diverse in nature than anticipated from the lipid raft hypothesis (Abankwa and Vogel, 2007). Cortical actin is also required to maintain spatial segregation of membrane domains by organizing fencing (submembraneous adapter) and picketing (transmembrane) molecules (Cheng and Miller, 2001; Suzuki et al., 2005). In addition, in some instances, cholesterol is not tolerated in the immediate vicinity of transmembrane proteins. Thus, cholesterol promotes picketing of membrane microdomains by transmembrane proteins and removal of cholesterol has the reverse effect. Disruption of the actin cytoskeleton abolished the agonist-induced shift to rapidly diffusing species of CRFR2. This observation argues for actin-supported anisotropy of the membrane. It is less clear why depletion or aggregation of cholesterol had a similar effect. The lipid raft hypothesis predicts that cholesterol extraction ought to accelerate diffusion, an effect which has previously been observed with the A_{2A}-adenosine receptor (Charalambous *et al.*, 2008), but it fails to account for the loss of agonist-induced shift to rapid diffusion of CRFR2 and why CRFR1 and CRFR2 should differ. Cholesterol may play a structural role for some GPCRs: in crystals prepared from metarhodopsin-I, cholesterol is trapped within the transmembrane core of the protein (Ruprecht *et al.*, 2004). Similarly, crystal packing of the β_2-adrenergic receptor is apparently facilitated by cholesterol (Cherezov et al., 2007).We therefore propose that the different response to agonist occupancy of CRFR1 and CRFR2 is accounted for by differences in the hydrophobic core of the two receptors, which affects their

ability to accommodate cholesterol. In spite of their high homology, the TM-segments of CRFR1 and CRFR2 show subtle differences: there is, for instance, an excess of bulky side chains in TM1 of CRFR1 (two isoleucines replacing valines) and the corresponding substitutions in TM4 of CRFR2. It is worth pointing out that the conformational change induced by agonist in CRFR2 caused a structural rearrangement large enough to affect FRET in CRFR2, while this was not the case in CRFR1. FIDA unequivocally demonstrated that this enhanced FRET was not due to a change in the oligomeric stoichiometry. Thus, CRFR2 and CRFR1 react to the same agonist and the same cognate G protein(s) with a subtle difference in conformation.

We noted that on average, CRFRs moved faster in hippocampal neurons (see Fig. 5) than in HEK293 cells (e.g. 5.8±3.4 and 9.7±4.5 × 10^{-9} cm^2/s for CRFR2 expressed in HEK 293 cells and in neurons, respectively). This was surprising, because neurons are thought to contain a large array of adapters linking membrane proteins to the cytoskeleton. Thus, picketing and fencing from the cytoskeleton is expected to be more pronounced in neuronal cells. However, it is worth noting that we examined the mobility of the receptors over the somatic region and that these neurons did not form extensive synapses. It is likely that picketing and fencing of some areas of the membrane requires synaptic input to organize the actin cytoskeleton. Large variations were also noted for the β_2-adrenergic receptor when expressed in A549 cells allowing for the resolution of two components (28.8±17.2 and 1.1±0.46 × 10^{-9} cm^2/s); importantly, the mobility of the β_2-adrenergic receptors was higher when expressed in hippocampal neurons than in A549 cells (Hegener et al., 2004). Most importantly, in hippocampal neurons, CRF again promoted a shift in the distribution of CRFR2 – but not of CRFR1- in favour of the rapidly migrating species. Thus, the variation in diffusion coefficients that we observed is likely representative of the possible range of mobility, which

Molecular Pharmacology Fast Forward. Published on September 15, 2009 as DOI: 10.1124/mol.109.059139
This article has not been copyedited and formatted. The final version may differ from this version.

occurs in the intact organism. We are also confident that the observations faithfully reproduce intrinsic differences in the response of the two receptor subtypes, which are important *in vivo.*

Molecular Pharmacology Fast Forward. Published on September 15, 2009 as DOI: 10.1124/mol.109.059139
This article has not been copyedited and formatted. The final version may differ from this version.

ACKNOWLEDGMENTS

We thank Helmut Kubista for help with the preparation of hippocampal neurons, Marion Holy for excellent technical assistance, Johannes A. Schmid for help with FRAP analysis and insightful comments.

Molecular Pharmacology Fast Forward. Published on September 15, 2009 as DOI: 10.1124/mol.109.059139
This article has not been copyedited and formatted. The final version may differ from this version.

References:

Abankwa D, Vogel H (2007) A FRET map of membrane anchors suggests distinct microdomains of heterotrimeric G proteins. *J Cell Sci* **120**:2953-2962

Adkins EM, Samuvel D J, Fog J U, Eriksen J, Jayanthi L D, Vaegter C B, Ramamoorthy S and Gether U (2007) Membrane mobility and microdomain association of the dopamine transporter studied with fluorescence correlation spectroscopy and fluorescence recovery after photobleaching. *Biochemistry* **46**:10484-10497.

Allen JA, Halverson-Tamboli RA, Rasenick MM (2007) Lipid raft microdomains and neurotransmitter signaling. *Nat Rev Neurosci* **8**:128–140

Bacia K and Schwille P (2003) A dynamic view of cellular processes by in vivo fluorescence auto- and cross-correlation spectroscopy. *Methods* **29**:74-85.

Barak LS, Ferguson S S G, Zhang J and Caron M G (1997) A β-arrestin green fluorescent protein biosensor for detecting G protein-coupled receptor activation. *J Biol Chem* **272**:27497-27500.

Bartholomaeus I, Milan-Lobo L, Nicke A, Dutertre S, Hastrup H, Jha A, Gether U, Sitte H H, Betz H and Eulenburg V (2008) Glycine transporter dimers: Evidence for occurrence in the plasma membrane. *J Biol Chem* **283**:10978-10991.

Briddon SJ, Middleton R J, Cordeaux Y, Flavin F M, Weinstein J A, George M W, Kellam B and Hill S J (2004) Quantitative analysis of the formation and diffusion of A_1-adenosine receptor-antagonist complexes in single living cells. *Proc Natl Acad Sci U S A* **101**:4673-4678.

Brock C, Oueslati N, Soler S, Boudier L, Rondard P and Pin J P (2007) Activation of a dimeric metabotropic glutamate receptor by intersubunit rearrangement. *J Biol Chem* **282**:33000-33008.

Charalambous C, Gsandtner I, Keuerleber S, Milan-Lobo L, Kudlacek O, Freissmuth M and Zezula J (2008) Restricted collision coupling of the A_{2A}-receptor revisited: evidence for physical separation of two signaling cascades. *J Biol Chem* **283**:9276-9288

Chen Y, Lagerholm B C, Yang B and Jacobson K (2006) Methods to measure the lateral diffusion of membrane lipids and proteins. *Methods* **39**:147-153.

Cheng ZJ and Miller LJ (2001) Agonist-dependent dissociation of oligomeric complexes of G protein-coupled cholecystokinin receptors demonstrated in living cells using bioluminescence resonance energy transfer. *J Biol Chem* **276**:48040-48047.

Cherezov V, Rosenbaum D M, Hanson M A, Rasmussen S G F, Thian F S, Kobilka T S, Choi H J, Kuhn P, Weis W I, Kobilka B K and Stevens R C (2007) High-resolution crystal structure of an engineered human β_2-adrenergic G protein coupled receptor. *Science* **318**:1258-1265.

Chini B and Parenti M (2004) G protein coupled receptors in lipid rafts and caveolae: how, when and why do they go there? *Journal of Molecular Endocrinology* **32**:325-338.

Cvejic S and Devi L A (1997) Dimerization of the δ-opioid receptor: implication for a role in receptor internalization. *J Biol Chem* **272**:26959-26964.

Edetsberger M, Gaubitzer E, Valic E, Waigmann E and Köhler G (2005) Detection of nanometer-sized particles in living cells using modern fluorescence fluctuation methods. *Biochemical and Biophysical Research Communications* **332**:109-116.

Ernst OP, Gramse V, Kolbe M, Hofmann K P and Heck M (2007) Monomeric G protein-coupled receptor rhodopsin in solution activates its G protein transducin at the diffusion limit. *Proc Natl Acad Sci U S A* **104**:10859-10864.

Fredriksson R, Lagerstrom M C, Lundin L G and Schioth H B (2003) The G protein-coupled receptors in the human genome form five main families. Phylogenetic analysis, paralogon groups, and fingerprints. *Mol Pharmacol* **63**:1256-1272.

Freissmuth M, Casey P J and Gilman A G (1989) G-Proteins control diverse pathways of transmembrane signaling. *Faseb Journal* **3**:2125-2131.

Haupts U, Maiti S, Schwille P and Webb W W (1998) Dynamics of fluorescence fluctuations in green fluorescent protein observed by fluorescence correlation spectroscopy. *Proc Natl Acad Sci U S A* **95**:13573-13578.

Head BP, Patel HH, Roth DM, Murray F, Swaney JS, Niesman IR, Farquhar MG, Insel PA (2006) Microtubules and actin microfilaments regulate lipid raft/caveolae localization of adenylyl cyclase signaling components. *J Biol Chem* **281**:26391-26399

Hegener O, Prenner L, Runkel F, Baader S L, Kappler J and Haberlein H (2004) Dynamics of β_2-adrenergic receptor - ligand complexes on living cells. *Biochemistry* **43**:6190-6199.

Hein P, Frank M, Hoffmann C, Lohse M J and Bunemann M (2005) Dynamics of receptor/G protein coupling in living cells. *EMBO J* **24**:4106-4114.

Hlavackova V, Goudet C, Kniazeff J, Zikova A, Maurel D, Vol C, Trojanova J, Prezeau L, Pin J P and Blahos J (2005) Evidence for a single heptahelical domain being turned on upon activation of a dimeric GPCR. *EMBO J* **24**:499-509.

Just H, Sitte H H, Schmid J A, Freissmuth M and Kudlacek O (2004) Identification of an additional interaction domain in transmembrane domains 11 and 12 that supports oligomer formation in the human serotonin transporter. *J Biol Chem* **279**:6650-6657.

Kask P, Palo K, Ullmann D and Gall K (1999) Fluorescence-intensity distribution analysis and its application in biomolecular detection technology. *Proc Natl Acad Sci U S A* **96**:13756-13761.

Kudlacek O, Mitterauer T, Nanoff C, Hohenegger M, Tang W J, Freissmuth M and Kleuss C (2001) Inhibition of adenylyl and guanylyl cyclase isoforms by the antiviral drug foscarnet. *J Biol Chem* **276**:3010-3016.

Maier C, Runzler D, Schindelar J, Grabner G, Waldhausl W, Kohler G and Luger A (2005) G-Protein-coupled glucocorticoid receptors on the pituitary cell membrane. *J Cell Sci* **118**:3353-3361.

Perez JB, Segura J M, Abankwa D, Piguet J, Martinez K L and Vogel H (2006) Monitoring the diffusion of single heterotrimeric G proteins in supported cell-membrane sheets reveals their partitioning into microdomains. *J Mol Biol* **363**:918-930.

Pfleger KD, Eidne KA (2005) Monitoring the formation of dynamic G-protein-coupled receptor-protein complexes in living cells. *Biochem J.* 385:625-37.

Philip F, Sengupta P and Scarlata S (2007) Signaling through a G protein-coupled receptor and its corresponding G protein follows a stoichiometrically limited model. *J Biol Chem* **282**:19203-19216.

Pin JP, Neubig R, Bouvier M, Devi L, Filizola M, Javitch J A, Lohse M J, Milligan G, Palczewski K, Parmentier M and Spedding M (2007) International Union of Basic and Clinical Pharmacology. LXVII. Recommendations for the recognition and nomenclature of G protein-coupled receptor heteromultimers. *Pharmacological Reviews* **59**:5-13.

Pucadyil TJ, Kalipatnapu S, Harikumar K G, Rangaraj N, Karnik S S and Chattopadhyay A (2004) G-protein-dependent cell surface dynamics of the human serotonin1A receptor tagged to yellow fluorescent protein. *Biochemistry* **43**:15852-15862.

Puthenveedu MA, von Zastrow M (2006) Cargo regulates clathrin-coated pit dynamics. *Cell* **127**:113-124.

Ruprecht JJ, Mielke T, Vogel R, Villa C and Schertler G F X (2004) Electron crystallography reveals the structure of metarhodopsin I. *EMBO J* **23**:3609-3620.

Suzuki K, Ritchie K, Kajikawa E, Fujiwara T and Kusumi A (2005) Rapid hop diffusion of a G-protein-coupled receptor in the plasma membrane as revealed by single-molecule techniques. *Biophys J* **88**:3659-3680.

Waldhoer M, Wise A, Milligan G, Freissmuth M, Nanoff C (1999) Kinetics of ternary complex formation with fusion proteins composed of the A(1)-adenosine receptor and G protein α-subunits. *J Biol Chem* **274**:30571-30579

Whorton MR, Bokoch M P, Rasmussen S G F, Huang B, Zare R N, Kobilka B and Sunahara R K (2007) A monomeric G protein-coupled receptor isolated in a high-density lipoprotein particle efficiently activates its G protein. *Proc Natl Acad Sci U S A* **104**:7682-7687.

Whetton AD, Gordon LM, Houslay MD (1983) Elevated membrane cholesterol concentrations inhibit glucagon-stimulated adenylate cyclase. Biochem J 210:437-449.

Wietfeld D, Heinrich N, Furkert J, Fechner K, Beyermann M, Bienert M and Berger H (2004) Regulation of the coupling to different G proteins of rat corticotropin-releasing factor receptor type 1 in human embryonic kidney 293 Cells. *J Biol Chem* **279**:38386-38394.

Yguerabide J, Schmidt J A and Yguerabide E E (1982) Lateral mobility in membranes as detected by fluorescence recovery after photobleaching. *Biophys J* **40**:69-75.

Molecular Pharmacology Fast Forward. Published on September 15, 2009 as DOI: 10.1124/mol.109.059139
This article has not been copyedited and formatted. The final version may differ from this version.

Footnotes:

This work was supported by the Austrian Science Fund/FWF [Grants P17076, P18706 to HHS and N209 to GK], the WWTF (MA 05 to GK) and the Gallo Research Institute and Clinics. IG is supported by a Doc-fforte stipend of the Austrian Academy of Sciences.

[1]Present address of Laura Milan-Lobo: The Ernest Gallo Clinic and Research Center, Emeryville, CA, USA

Molecular Pharmacology Fast Forward. Published on September 15, 2009 as DOI: 10.1124/mol.109.059139
This article has not been copyedited and formatted. The final version may differ from this version.

LEGENDS FOR FIGURES

Fig. 1. **Accumulation of cAMP in HEK293 cells expressing CRF-receptors.** Bell-shaped concentration-response curve for CRF-induced cAMP accumulation in HEK293 cells stably expressing the YFP-tagged versions of CRFR1 (Panel A) or of CRFR2 (Panel B). The adenine nucleotide pool of stably transfected HEK293 cells (2×10^5/well) was metabolically prelabeled with [^{3}H]adenine for 16h; where indicated (triangles), cells were also maintained in the presence of pertussis toxin (100 ng/mL). Thereafter the cells were preincubated in the presence of rolipram (100 μM) for 1 h and subsequently stimulated with the indicated concentrations of CRF for 30min. The accumulation of [^{3}H]cAMP was quantified as outlined under Materials and Methods. In order to normalize for interassay variations, the maximum cAMP accumulation (observed with 6 nM and 10 nM in cells expressing CRFR1-Y and CRFR2-Y, respectively) was set 100%. This value corresponded to 6295±688 cpm and 2389±176 cpm for CRFR1-Y and CRFR2-Y, respectively. Basal [^{3}H]cAMP levels were 71±15 cpm and 108±7 cpm for CRFR1-Y and CRFR2-Y, respectively. Data represent means±SEM; n=3-8 experimental days, each concentration point measured in triplicates.

Fig. 2. **FRET microscopy of CRF-receptors**. (A) HEK293 cells transiently expressed plasmids encoding CFP or YFP tagged proteins as indicated. The columns show CFP and YFP images as indicated, the third column shows a false-color rendering of the bleed-through corrected FRETc image. All images are representative of 2-7 experimental days and corrected for background. Scale bar=10 μm. (B) N_{FRET}-values were calculated as described (6); cells expressed the indicated constructs: ECFP + EYFP (n=106 cells), CRFR2-C + Y-DAT (n=13), CRFR1-C + Y-DAT (n=11), CRFR2-C + CRFR1-Y (n=39), CRFR2-C + CRFR2-Y (n=220), CRFR1-C + CRFR1-Y (n=90) and C-SERT-Y (n=124). (C) N_{FRET}–values were determined in cells expressing the indicated CRFR-isoforms: CRFR2-C and CRFR2-Y in the absence

Molecular Pharmacology Fast Forward. Published on September 15, 2009 as DOI: 10.1124/mol.109.059139
This article has not been copyedited and formatted. The final version may differ from this version.

(n=220 cells) and presence of CRF (10 nM, n=103; 100 nM, n=83), similarly, CRFR1-C and CRFR1-Y in the absence (n=90) and presence of CRF (10 nM, n=27; 100 nM, n=26).

Fig. 3. **CRFRs interact with β-Arrestin and internalize upon agonist treatment.** (A) HEK293 cells transiently expressed plasmids encoding CFP-tagged CRFRs or YFP tagged β-arrestin-1. FRET microscopy was performed in the absence (open bars) or presence of agonist CRF (filled bars; [CRF] 100 nM) as described in "Material and Methods"; NFRET-values were determined as described (6). Data represent means ± SEM (n = 7, two independent transfections). (B) Confocal images of HEK293 co-transfected with either CRFR1 or CRFR2 tagged with YFP (displayed in green color) and Rab5 tagged with CFP (displayed in red color). Yellow colouring indicates co-localization of YFP- and CFP-tagged proteins (at control conditions and after incubation with 100 nM CRF at the times indicated). The images are representative of three experimental days. The colocalization of CRFRs and of rab5 was scored by an observer blinded to the experimental condition. 6 to 11 cells from different experiments were scored/time point. The resulting average density of receptor positive vesicle/optical section of a given cell was plotted as a function of time. Error bars represent SEM.

Fig. 4. **FRAP microscopy of CRF-receptors**. (A) Confocal images of stably transfected HEK293-CRFR1-Y or HEK293-CRFR2-Y cells, representative of 3-6 experimental days. After an initial cell scan (0 s), a region of interest (arrow) was photobleached and the recovery of the fluorescence monitored over 90 sec. The normalized fluorescence recovery was plotted versus time as an example of one experimental day and fitted by non-linear regression (see materials and methods; basal: n=9, 10 nM CRF: n=7 and 100 nM CRF: n=7, 10 μM of antagonist αhCRF[9-41]: n=11). The length of the photobleached strip was 5.5±0.4 μm. (B) Scatter plots of the diffusion coefficients (n=20-30 cells for CRFR1; n=21-88 cells for

Molecular Pharmacology Fast Forward. Published on September 15, 2009 as DOI: 10.1124/mol.109.059139
This article has not been copyedited and formatted. The final version may differ from this version.

CRFR2). (C) Scatter plots of the mobile fractions for each receptor subtype under the same conditions described before. Horizontal lines represent the mean. ***P*<0.01 and ****P*<0.001; n.s. not significant. Scale bar 10μm.

Fig. 5. **FCS recordings of CRFRs stably expressed in HEK293 cells**. (A) Representative recordings of the intensity fluctuations (top panels) of CRFR1-Y and CRFR2-Y in the absence (black curve, a) and presence of 100 nM CRF (grey curve, b). Autocorrelation curves (lower panel) calculated from the intensity fluctuations (in kHz) were fitted to a two-component model and normalized (raw count rates; control conditions: CRFR1-Y= 238 kHz, CRFR2-Y=239 kHz; 100 nM CRF: CRFR1-Y=131 kHz, CRFR2-Y=170 kHz). Under control conditions, the two components have diffusion times of τ1 ~0.13 ms and τ2 ~15.6 ms for CRFR1-Y cells and τ1 ~0.15 ms and τ2 ~20.5 ms for CRFR2-Y cells. (B) Scatter plots represent the diffusion coefficient of both CRFRs after incubation (15 min) in the absence and presence of CRF or 10 μM antagonist (αhCRF[9-41]); 3-13 experimental days, n=41-140 cells. Horizontal lines represent the mean; **P*<0.05, ***P*<0.01 and ****P*<0.001; n.s. not significant.

Fig. 6. **FCS recordings of CRFRs expressed in hippocampal neurons**. (A) Representative measurements of the intensity fluctuations (top two panels) of YFP-tagged CRFR1 and CRFR2 in transiently transfected hippocampal neurons. The measurements were done in the absence (black curve, a) and presence of 100 nM CRF (grey curve, b) and are representative of 3 experimental days. Autocorrelation curves (lower panel) were calculated from the intensity fluctuations (kHz); the curves were fitted to a two component-model and normalized (raw count rates; control conditions: CRFR1-Y=11 kHz, CRFR2-Y= 8 kHz; 100 nM CRF: CRFR1-Y=4kHz, CRFR2-Y=2.5kHz). The two components have diffusion times of τ1 ~0.013 ms and τ1 ~8.1 ms for CRFR1 control cells and τ1 ~0.018 ms and τ2 ~10.6 ms for

Molecular Pharmacology Fast Forward. Published on September 15, 2009 as DOI: 10.1124/mol.109.059139
This article has not been copyedited and formatted. The final version may differ from this version.

CRFR2 control cells. (B) Bar chart represents the diffusion coefficient of each receptor subtype at different concentrations of CRF; n=30-62.

Fig. 7. FCS-recordings in HEK293 cell lines expressing different levels of CRFR2. (A) Representative measurements of the intensity fluctuations (top panels) of three cell lines stably expressing CRFR2-Y (denoted #1 to #3). Autocorrelation curves (lower panel) were calculated from the intensity fluctuations (kHz) and fitted to a two component model. The right hand panel shows that the curves were superimposable. (B) Receptor levels visualized by immunblotting; lysates (~7 µg protein) were prepared from the three cell lines (#1 to #3) used in Panel A and from the CRFR1 expressing cell (#4) for comparison; after separation on a denaturing SDS-polyacrylamide gels, proteins were electrophoretically transferred onto nitrocellulose membranes, stained with Ponceau-S (right hand panel) and the immunoreactivity was subsequently visualized with an anti-GFP antibody (1:5000) by enhanced chemiluminescence using three different exposure times (indicated under each blot) to account for the large difference in expression levels. Note that differnces in loading do not account for the different levels of immunoreactivity. The full and empty arrows indicate immunoreactivity for CRFRs and free YFP, respectively. Data are from one representative experiment that has been replicated with identical results.

Fig. 8. **Mobility of CRFR2-Y after disruption of cortical actin and cholesterol depletion/clustering assessed by FCS**. (A) Representative measurement of the intensity fluctuations (top panels) of CRFR2-Y cells and after treatment with latrunculin A (1 µM), MβCD (8 mM) and filipin3 (5 µg/ml). Autocorrelation curves (lower panel) calculated from the intensity fluctuations (kHz) were fitted to a two component model yielding diffusion times of CRFR2 τ2: ~20.5, ~22, ~31.6 and ~92.5 ms for control, latrunculin A-, MβCD- and

Molecular Pharmacology Fast Forward. Published on September 15, 2009 as DOI: 10.1124/mol.109.059139
This article has not been copyedited and formatted. The final version may differ from this version.

filipin3-treated cells, respectively. (B) Scatter plots represent the diffusion coefficient of CRFR2-Y after incubation with CRF, latrunculin A (n=70), MβCD (n=20) or filipin3 (n=19). Horizontal lines represent the mean; $^{**}P<0.01$ and $^{***}P<0.001$; n.s. not significant.

Fig. 9. **CRFR complexes examined by FIDA.** (A) Representative measurements of the intensity fluctuations (kHz) detected by FCS (top panels) of CRFR1-Y and CRFR2-Y were used to calculate the probability of the photons detected by the microscope per 40 μs. A photon counting histogram is shown for CRFR1-Y and CRFR2-Y in the presence or absence of 100nM CRF. All measurements were best fitted with a single component model and the brightness of each was determined as described in Material and Methods. (B) Bar chart representing the brightness calculated for CRFR1-Y and CRFR2-Y at control conditions and 100nM CRF of (2 experimental days). Bars represent means±SEM, n=18-25 cells.

Fig. 10. **Time course of [^{125}I]sauvagine binding to membranes prepared from CRFR1 and CRFR2 expressing cells at different temperatures**. Panel A: Membranes from HEK293 cells expressing CRFR1 (2-4 μg/assay) were incubated for the indicated time intervals and at the indicated temperatures in the presence of 0.2 nM [^{125}I]sauvagine. A parallel incubation contained 0.1 mM GTPγS (open triangle), which reduced binding to a similar extent at all temperatures studied. Data are means±SD from three independent experiments carried out in duplicate. A similar experiment was also doen at 30°C but the points were omitted for the sake of clarity. The solid lines were drawn by fitting the data points to an equation describing a monoexponential association. Panel B: **Arrhenius plot.** Apparent on rates determined were obtained as outlined in panel A for CRFR1.

Molecular Pharmacology Fast Forward. Published on September 15, 2009 as DOI: 10.1124/mol.109.059139
This article has not been copyedited and formatted. The final version may differ from this version.

Fig. 11. **cAMP accumulation induced by CRFR1 and CRFR2 expressed at different levels (Panels A&B) and after pretreatment of HEK293 cells with latrunculin (Panels C&D).**

Panels A & B: HEK 293 cells ($6x10^6$ cells) were transiently transfected with 0.8 (closed symbol) or 4 µg plasmid (open symbol) encoding YFP-tagged CRFR1 (A) or CRFR2 (B). Cells ($3x10^5$ cells/6-well dish) were seeded 24 h after transfection and allowed to adhere for 8 h. Subsequently the cells were incubated in medium containing pertussis toxin (100 ng/mL) and [^{3}H]adenine (1 µCi/mL) overnight. Cells were subsequently stimulated with CRF for 20 min and the formation of [^{3}H]cAMP was quantified as outlined in the legend to Fig. 1. EC_{50}-values were (means±SD): 0.56±0.11 and 0.12±0.07 nM for low and high CRFR1 expression, respectively (p=0.0027; t-test for paired data); 0.29±0.10 and 0.21±0.05 for low and high CRFR2 expression, respectively (p=0.10; t-test for paired data). Panels C& D: Stably transfected HEK293 cells expressing CRFR1 (C) or CRFR2 (D) were prelabelled with [^{3}H]adenine overnight and then pretreated with latrunculin A as in Fig. 7 for 1 h prior to addition of agonist for 20 min. EC_{50}-values for CRF were 0.21±0.05 and 0.22±0.08 (CRFR1; p= 0.92) and 0.21±0.04 and 0.14±0.03 nM (CRFR2; p=0.04). Data points represent mean values ± SD from 3 (Panels A& B) and 5 (Panels C & D) independent experiments (done in triplicate); maximal [^{3}H]cAMP accumulation in each experiment was set 100% to account for interassay variation. These 100% values varied from 600 cpm (low receptor expression) to 5000 cpm (stable cell lines expressing CRFR1).

Fig. 12. **Agonist-induced internalization of CRFR1 and of CRFR2 in the presence or absence of latrunculin A.** HEK293 cells stably expressing CRFR1 or CRFR2 tagged with YFP were seeded on cover slips and pretreated with vehicle or latrunculin (row labeled + Latr.) as in Fig. 8. Images were captured under basal conditions (time point 0 minutes) using the 514 nm laser line of a Zeiss 501 confocal laser scanning microscope (see "Material and

Molecular Pharmacology Fast Forward. Published on September 15, 2009 as DOI: 10.1124/mol.109.059139
This article has not been copyedited and formatted. The final version may differ from this version.

Methods" section). Subsequently, CRF was added in a concentration of 100 nM and images captured in intervals of 10 minutes, in the presence or absence of latrunculin A. Laser power was set to 6 % with the exception of row "CRF2R Basal": here, laser intensity was set to 11 % to visualize all possible intracellular fluorescent particles. Shown are representative of images captured in parallel in the same experiment (and replicated with three cover slips, each); the experiment was repeated twice.

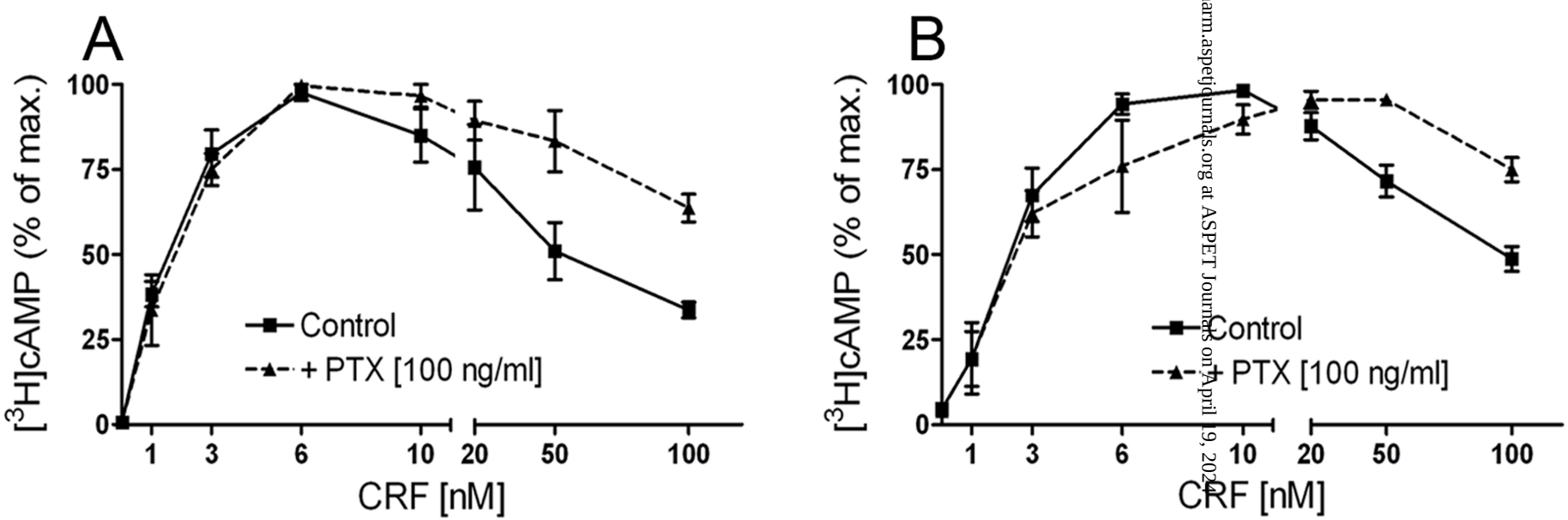

Fig. 1

Molecular Pharmacology Fast Forward. Published on September 15, 2009 as DOI: 10.1124/mol.109.059139
This article has not been copyedited and formatted. The final version may differ from this version.

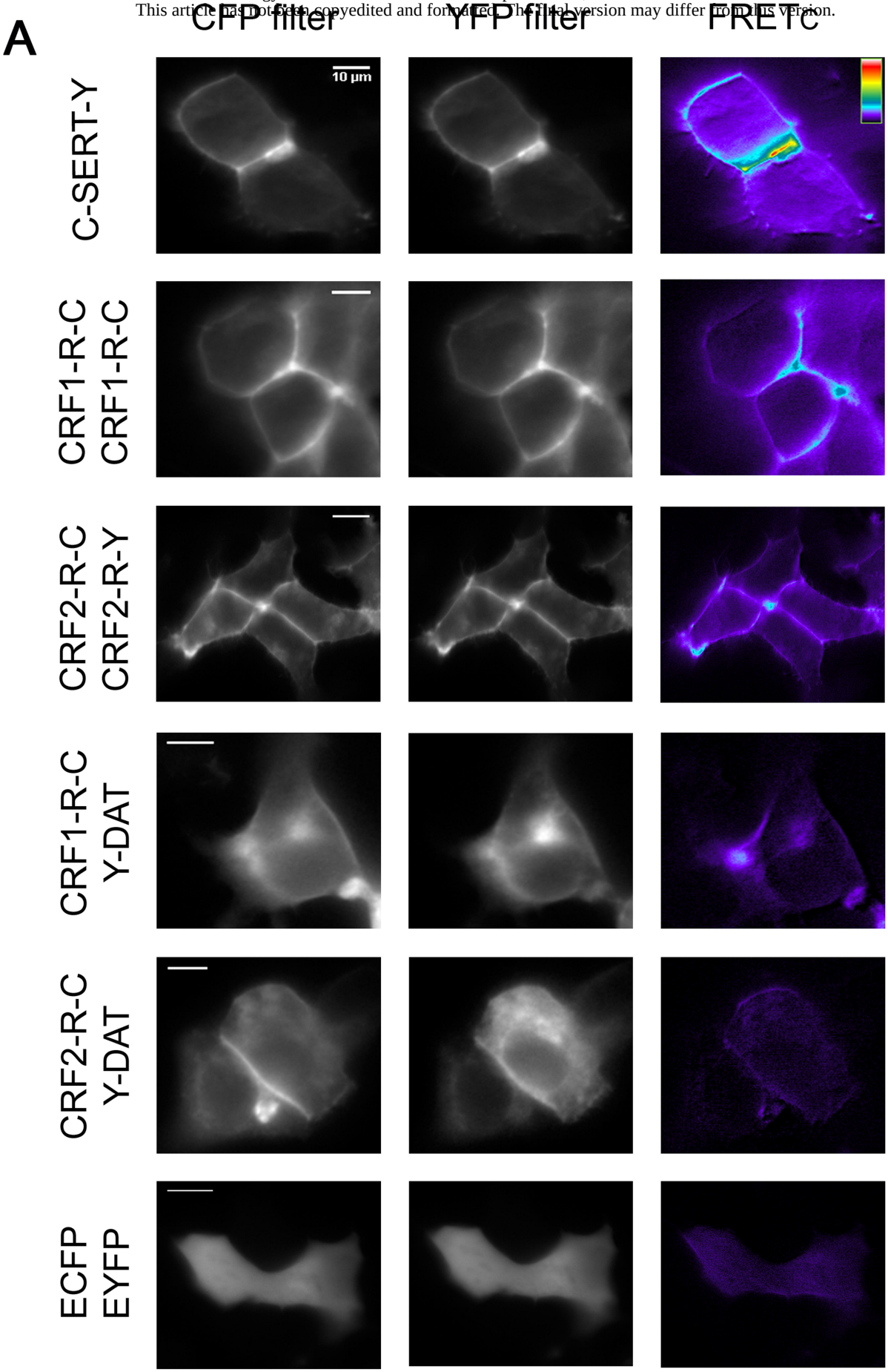

Fig. 2

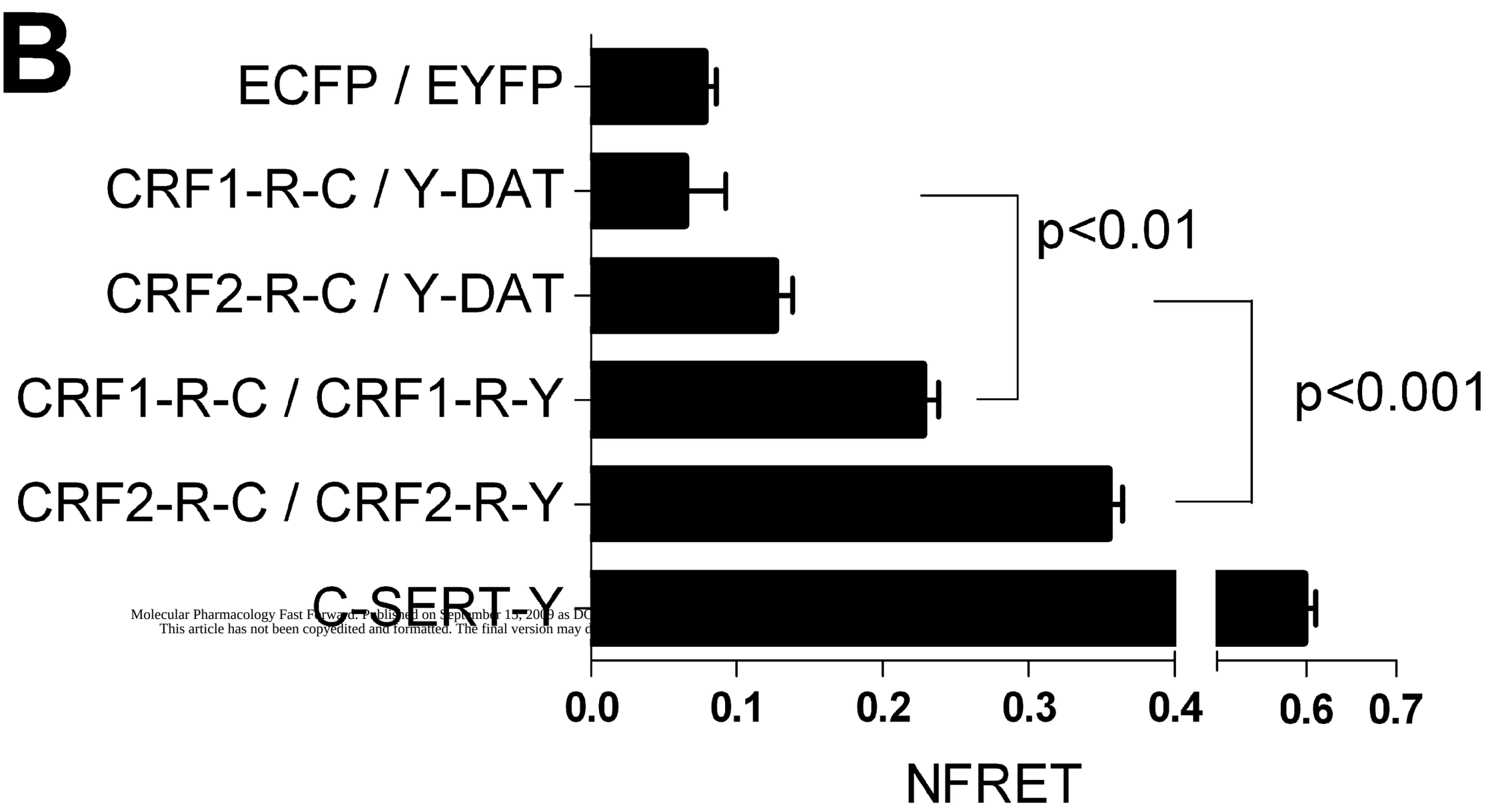

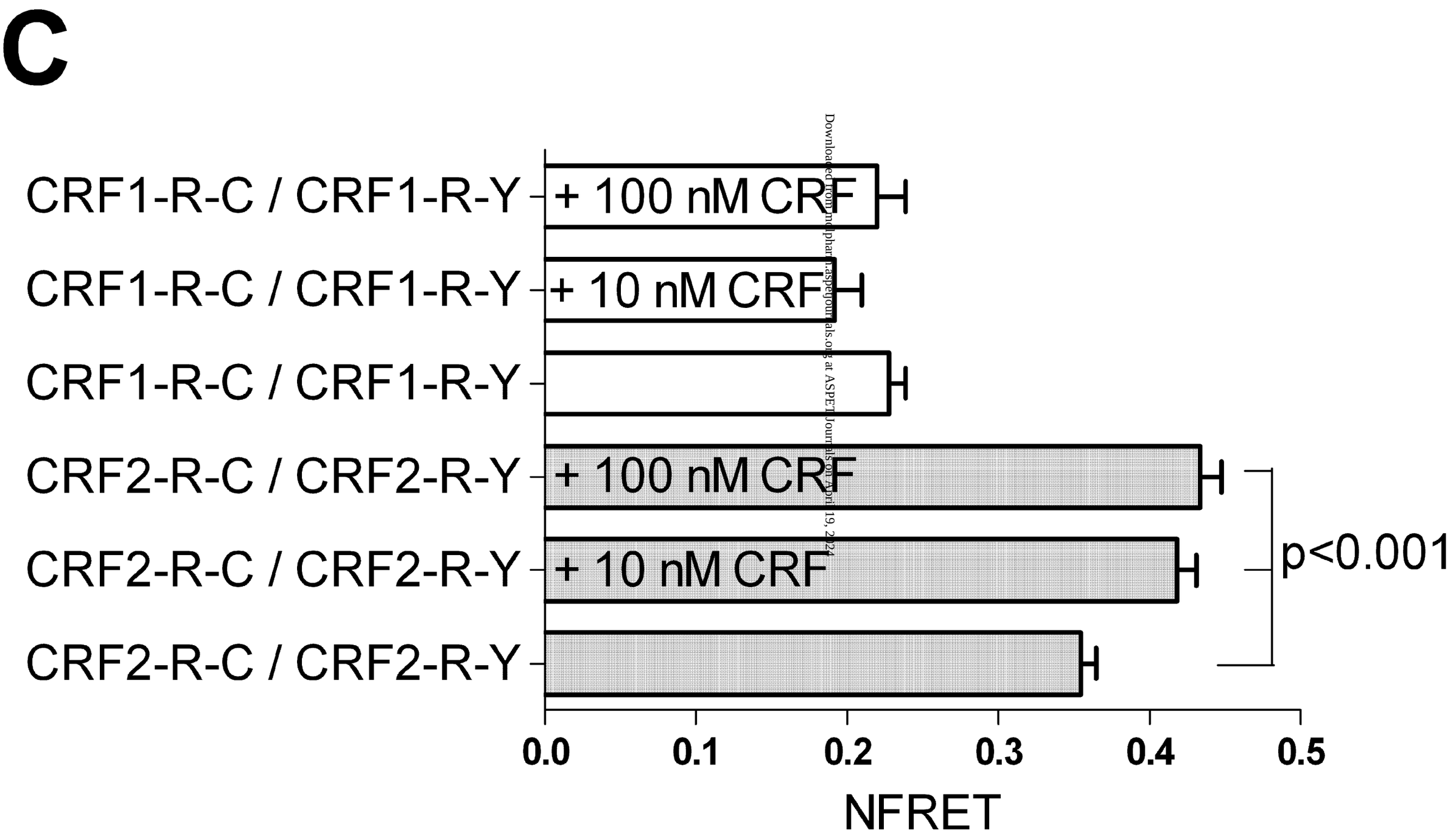

Molecular Pharmacology Fast Forward. Published on September 15, 2009 as DOI: 10.1124/mol.109.059139
This article has not been copyedited and formatted. The final version may differ from this version.

Fig. 3

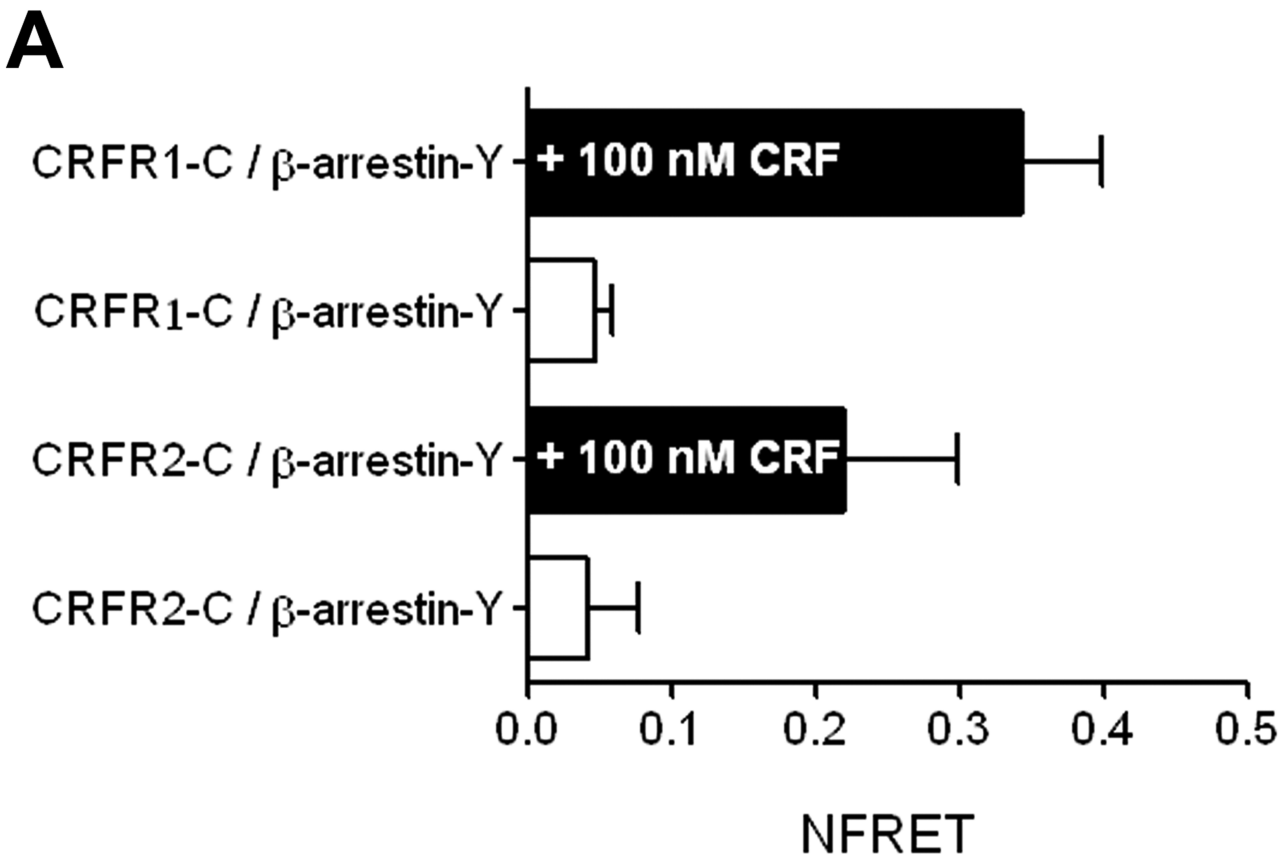

Molecular Pharmacology Fast Forward. Published on September 15, 2009 as DOI: 10.1124/mol.109.059139
This article has not been copyedited and formatted. The final version may differ from this version.

Fig. 3

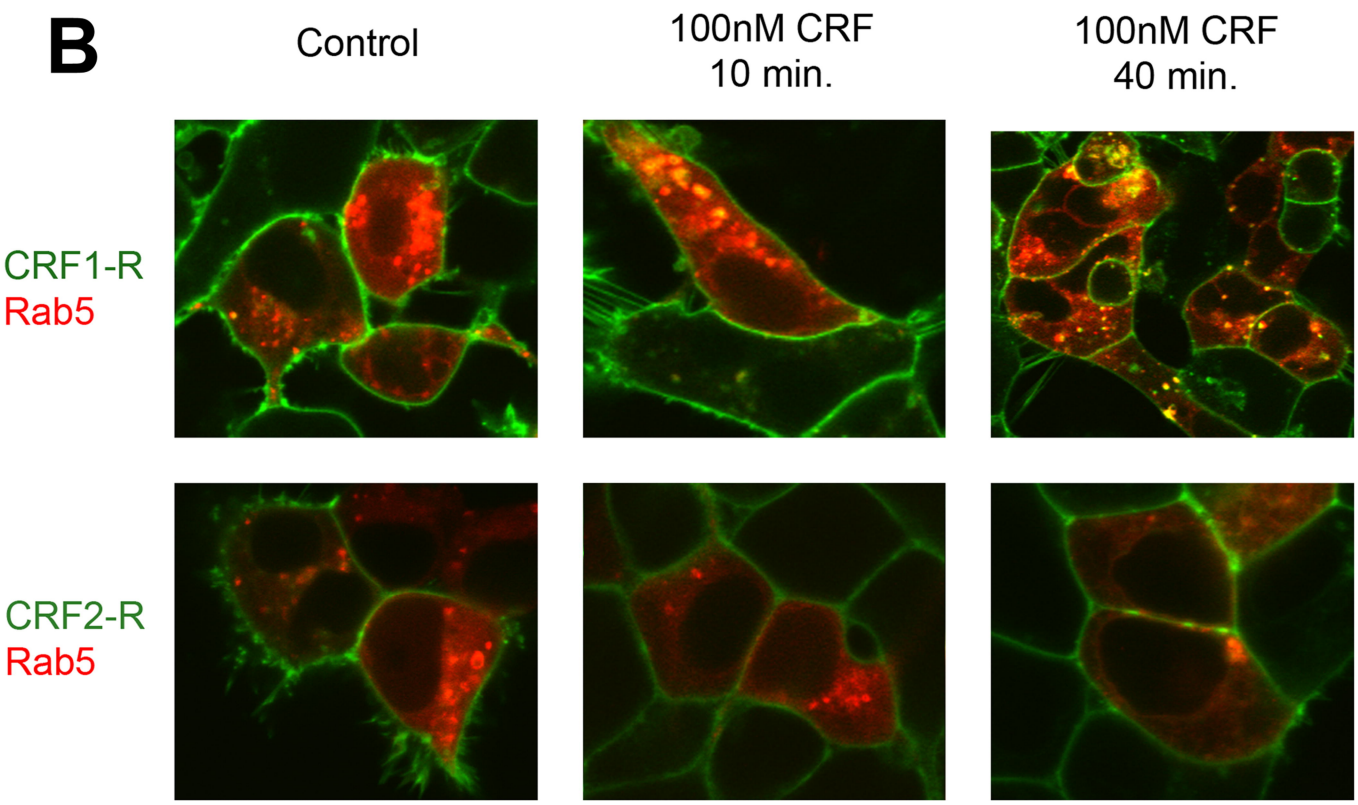

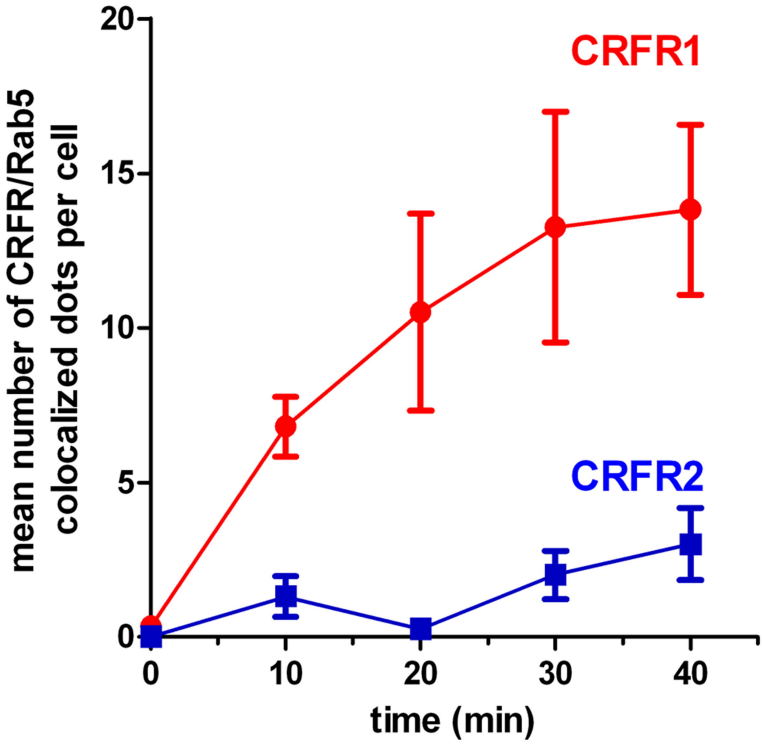

Fig. 4

Molecular Pharmacology Fast Forward. Published on September 15, 2009 as DOI: 10.1124/mol.109.059139
This article has not been copyedited and formatted. The final version may differ from this version.

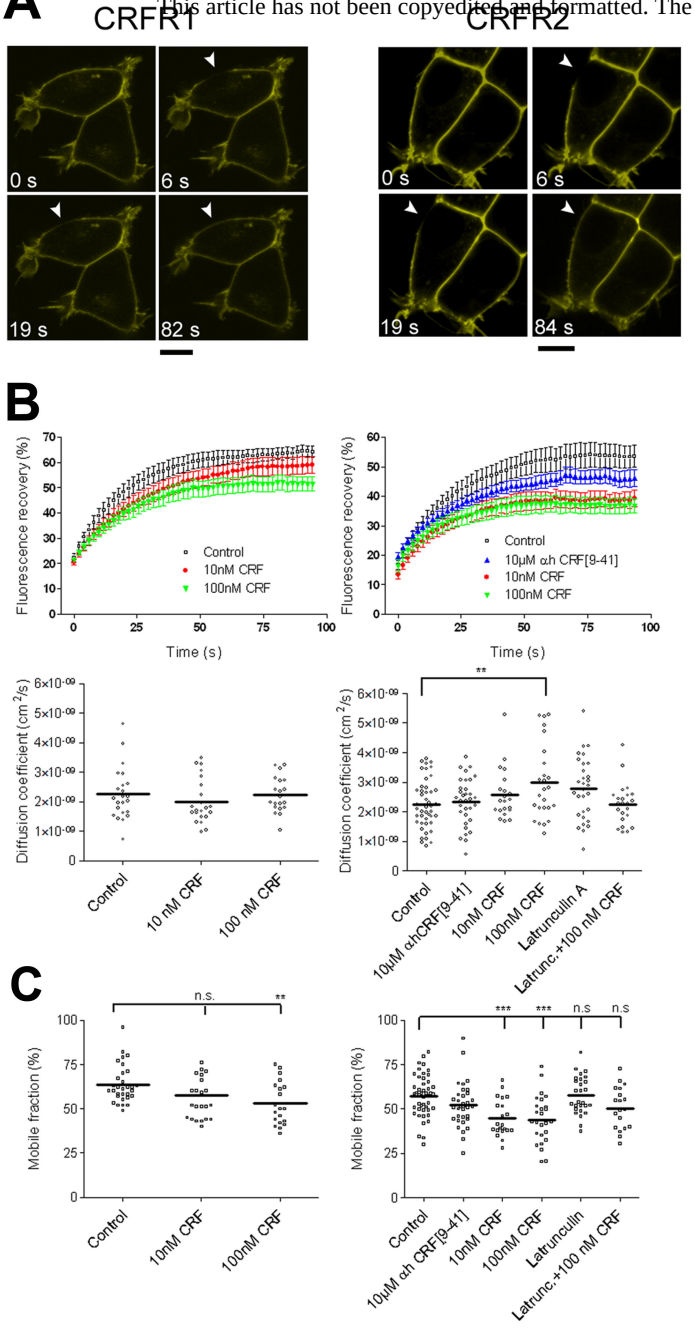

Fig. 5

Molecular Pharmacology Fast Forward. Published on September 15, 2009 as DOI: 10.1124/mol.109.059139
This article has not been copyedited and formatted. The final version may differ from this version.

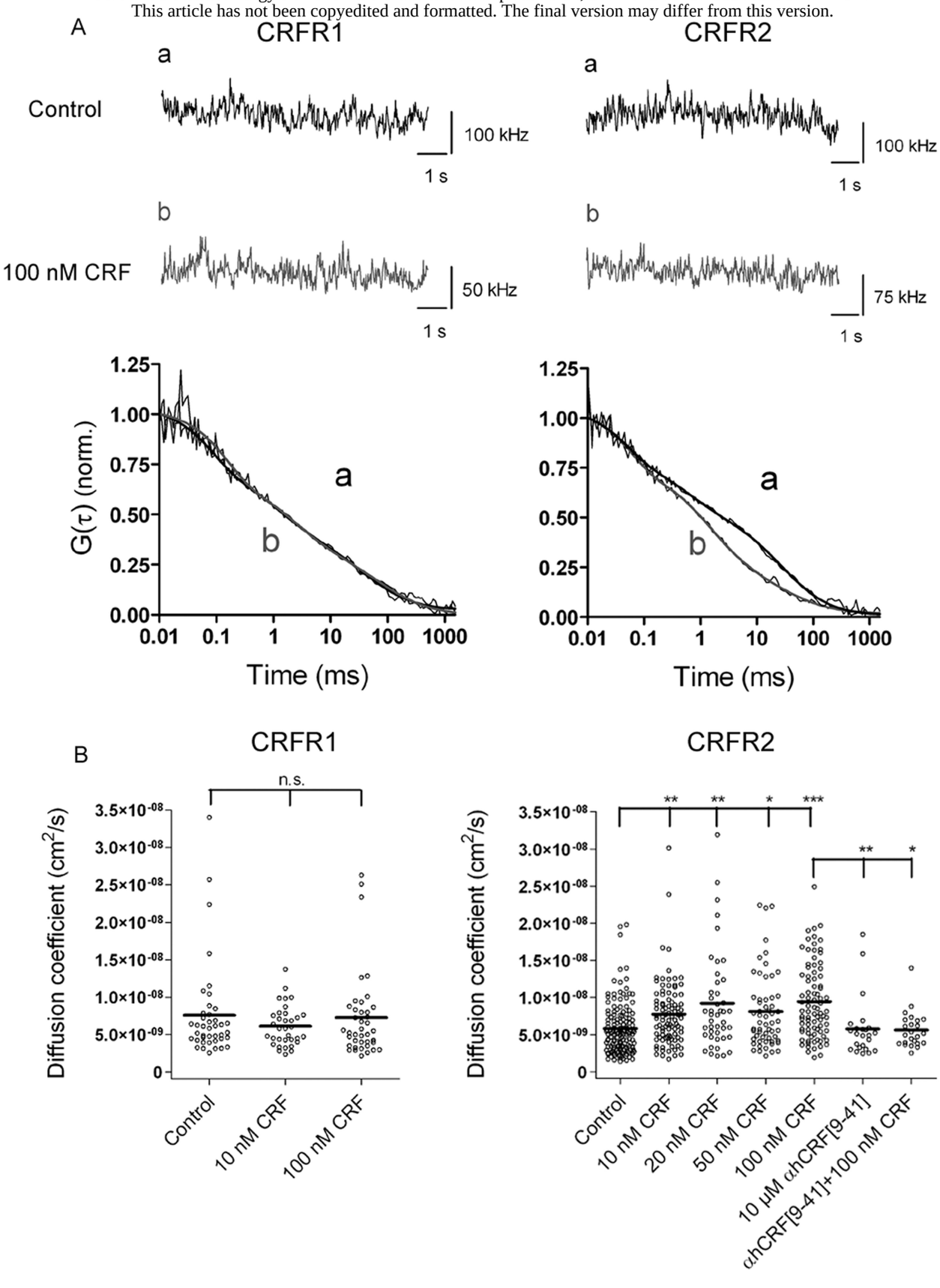

Fig. 6

Molecular Pharmacology Fast Forward. Published on September 15, 2009 as DOI: 10.1124/mol.109.059139
This article has not been copyedited and formatted. The final version may differ from this version.

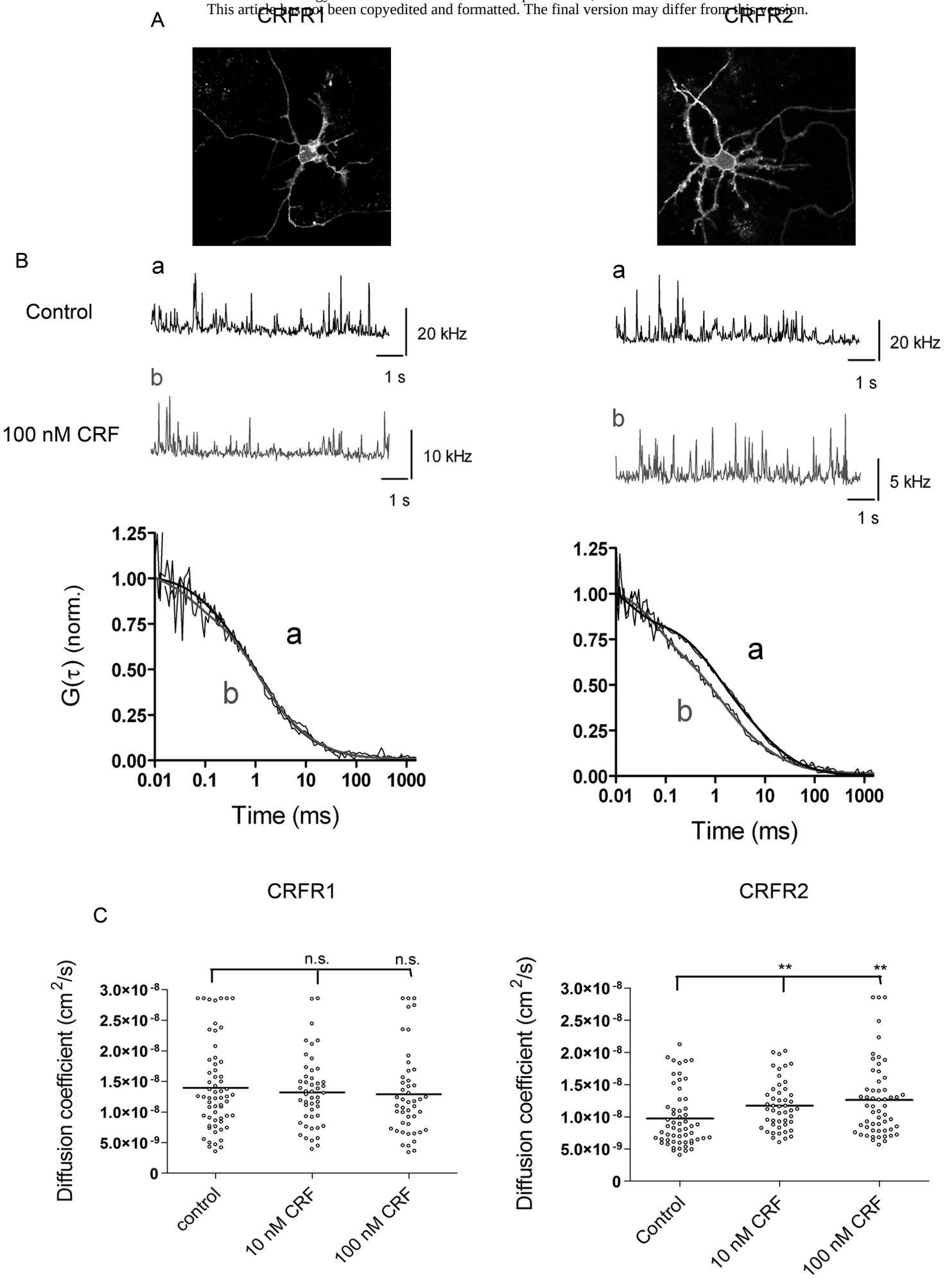

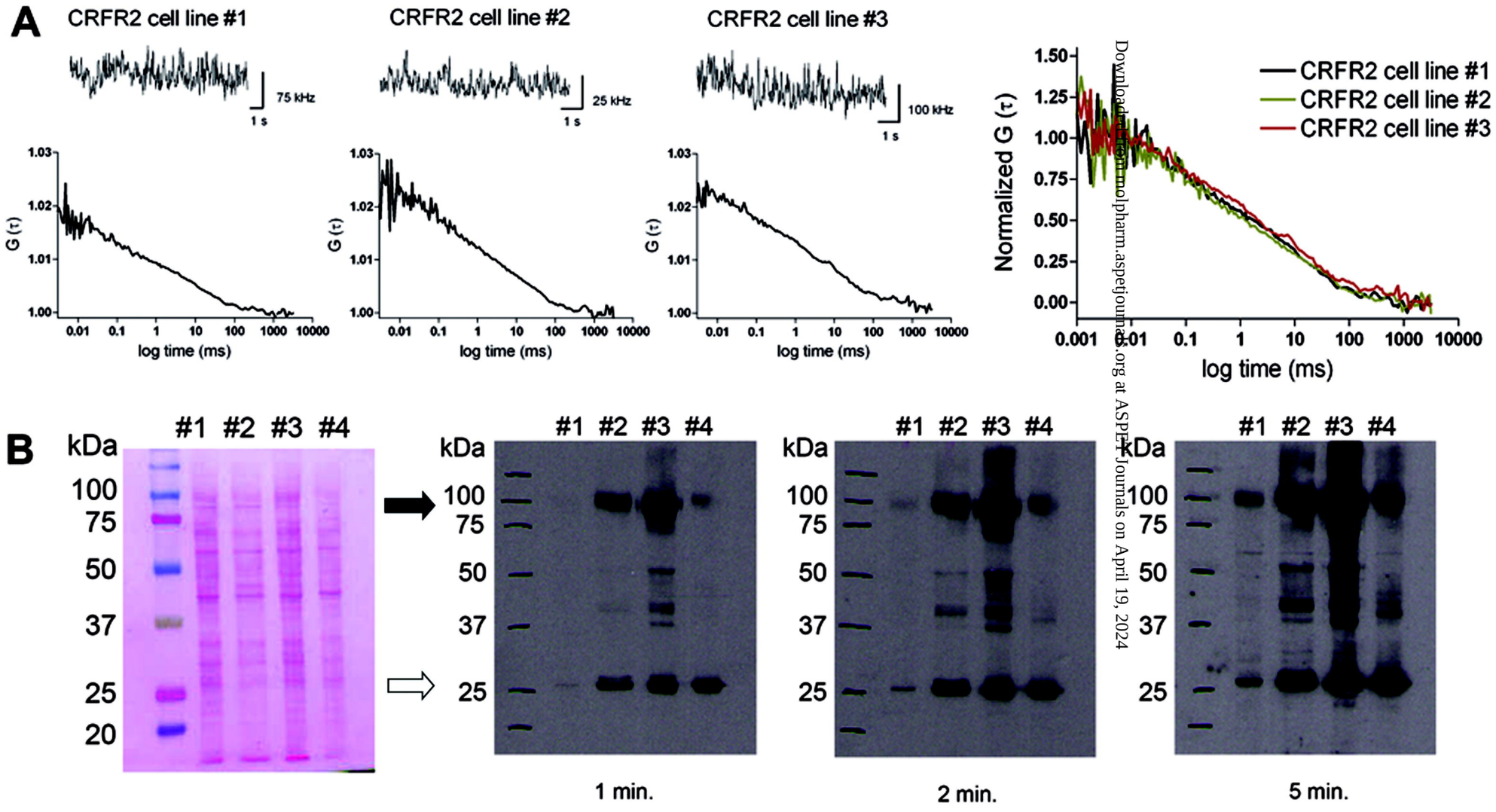

Fig. 7

Molecular Pharmacology Fast Forward. Published on September 15, 2009 as DOI: 10.1124/mol.109.059139
This article has not been copyedited and formatted. The final version may differ from this version.

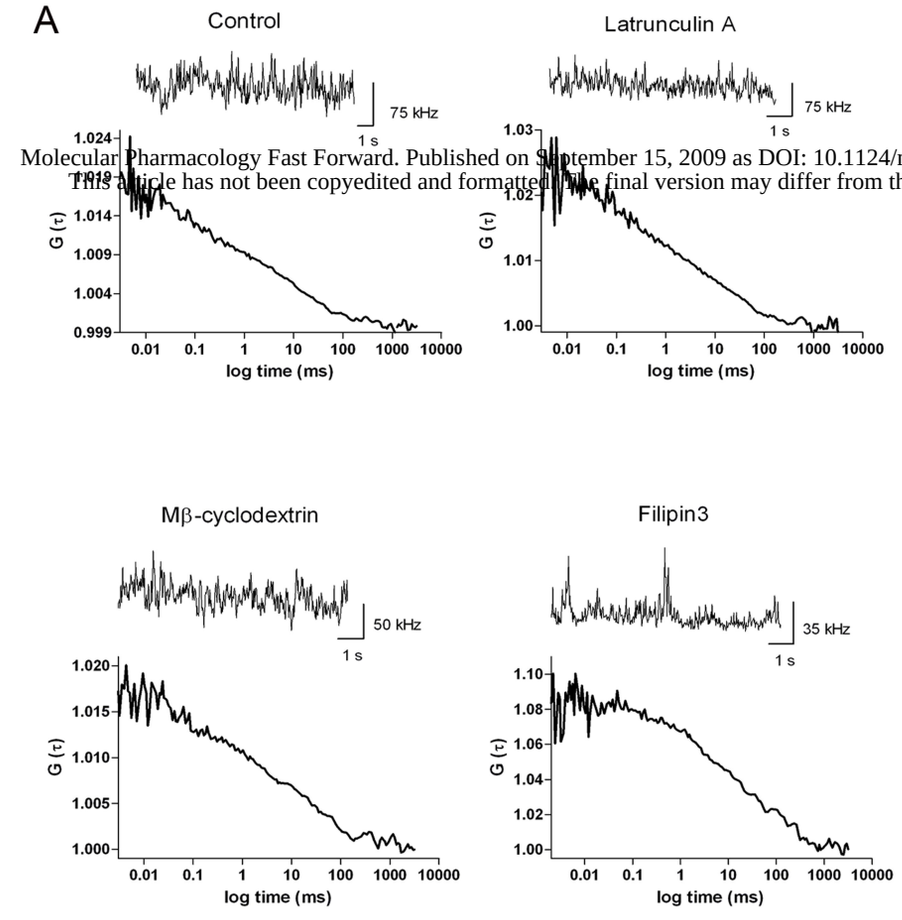

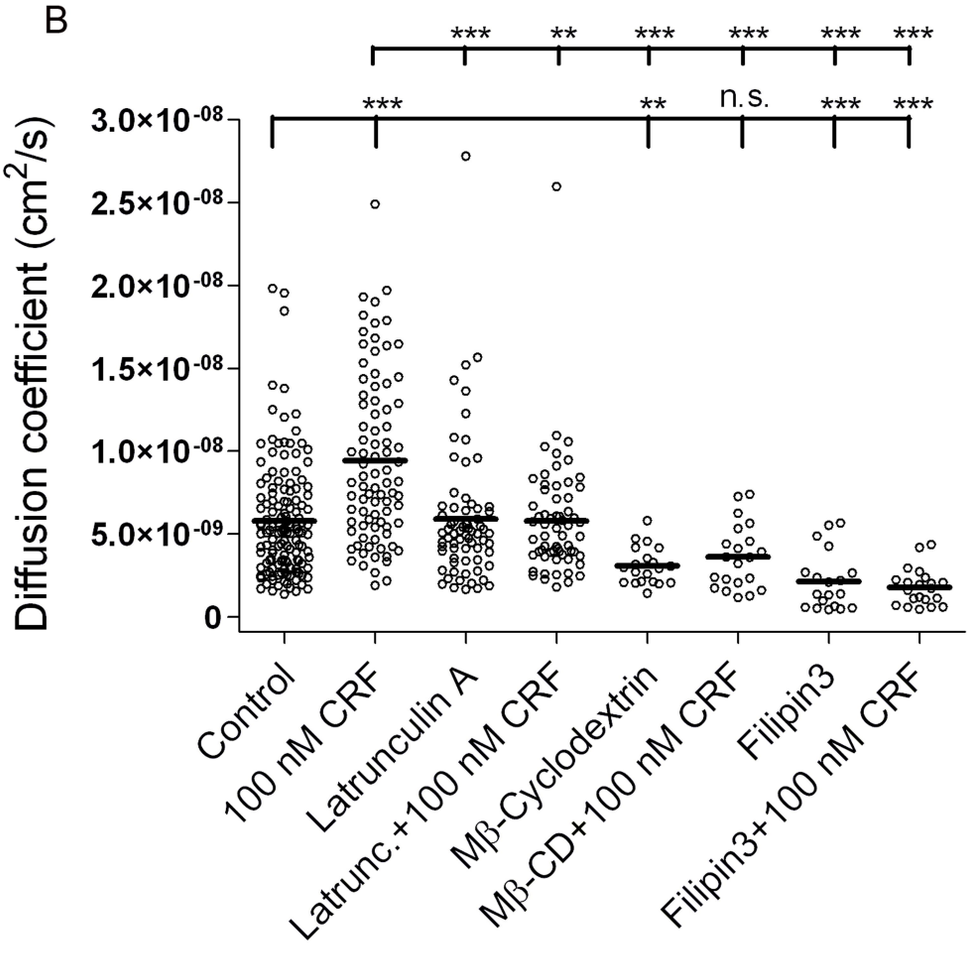

Fig. 8

Fig. 9

Molecular Pharmacology Fast Forward. Published on September 15, 2009 as DOI: 10.1124/mol.109.059139

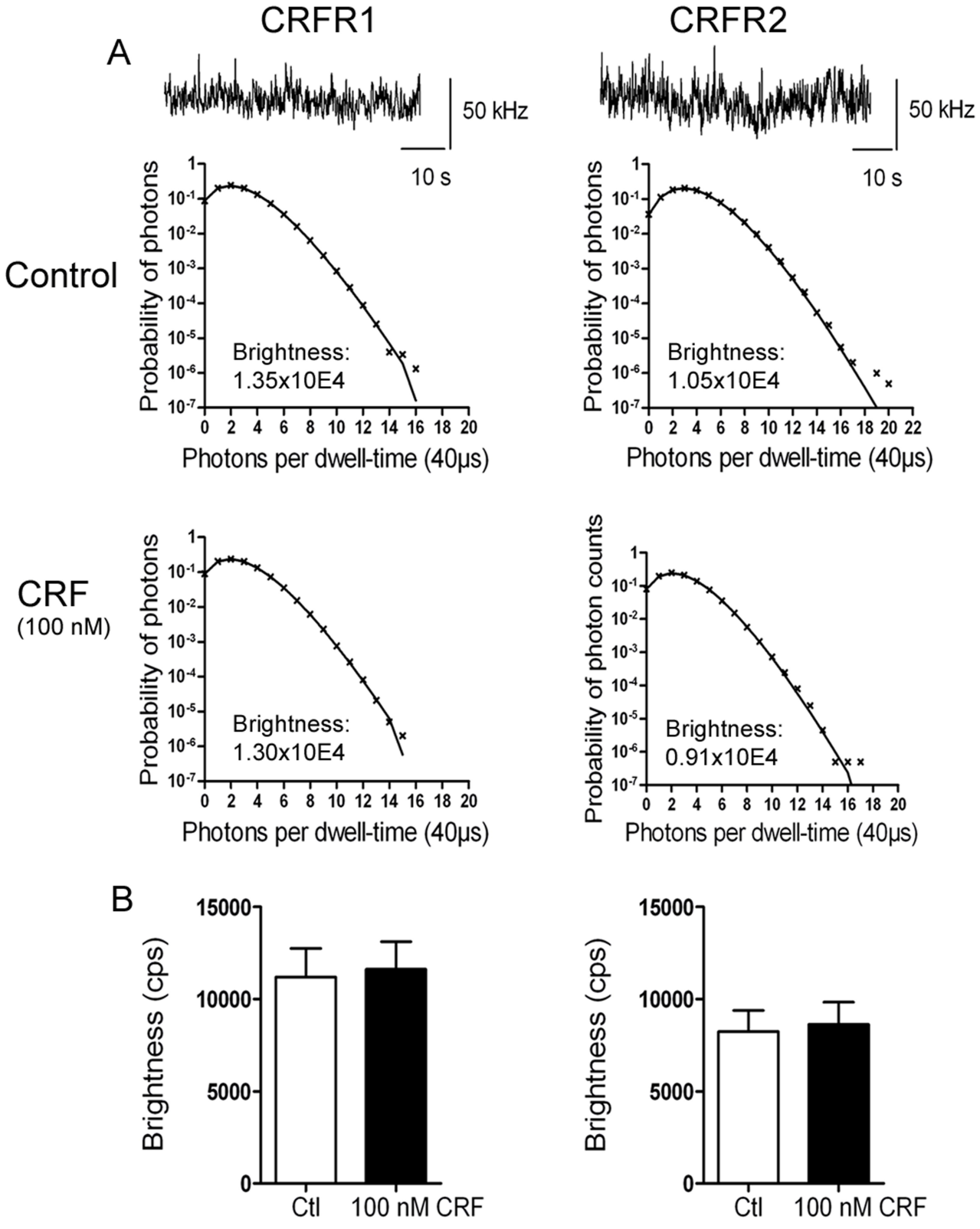

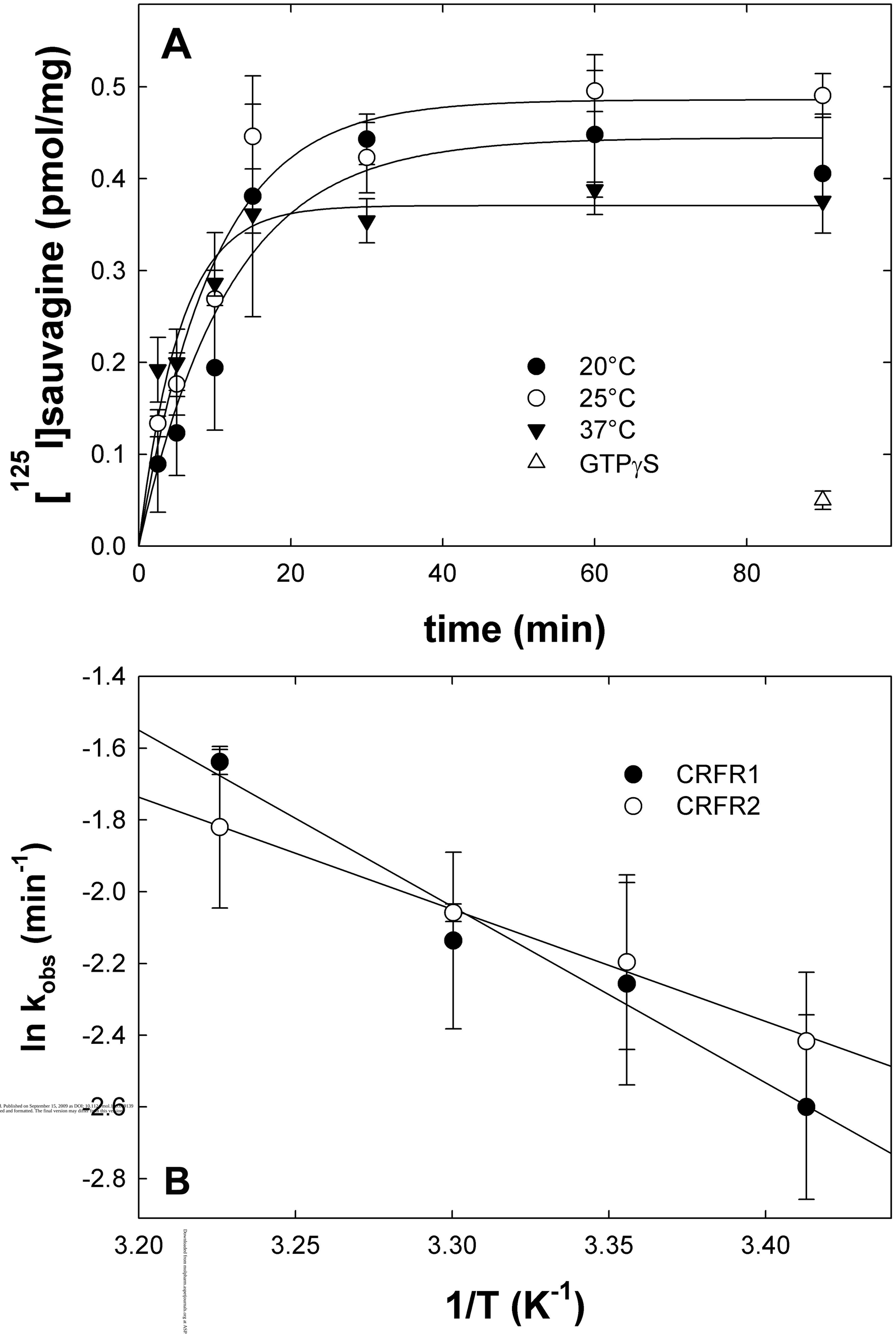

Fig. 10

Molecular Pharmacology Fast Forward. Published on September 15, 2009 as DOI: 10.1124/mol.109.059139
This article has not been copyedited and formatted. The final version may differ from this version.

Fig. 11

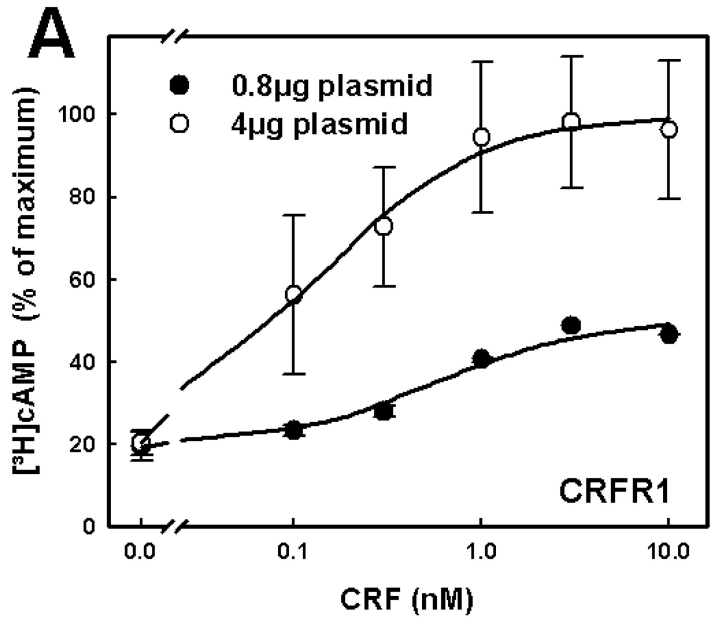

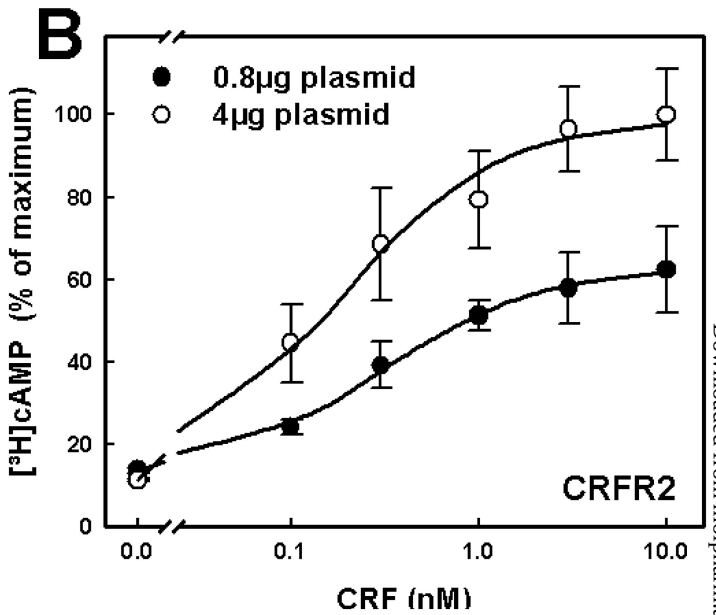

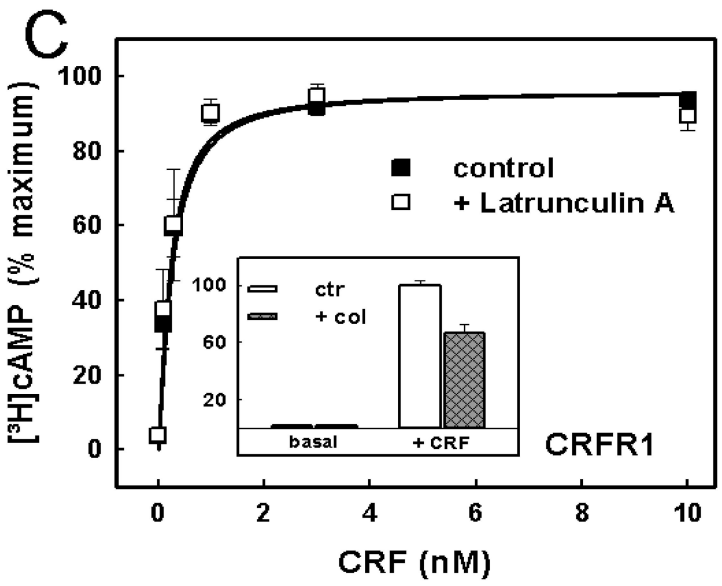

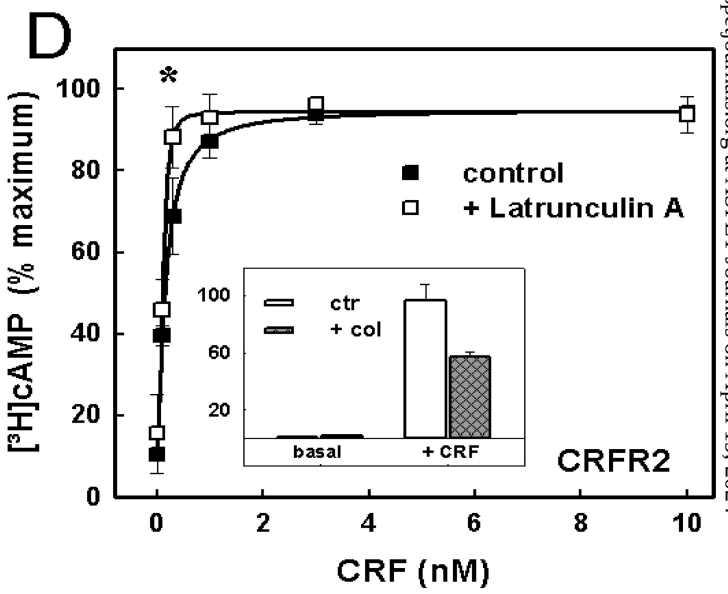

Molecular Pharmacology Fast Forward. Published on September 15, 2009 as DOI: 10.1124/mol.109.059139
This article has not been copyedited and formatted. The final version may differ from this version.

Fig. 12